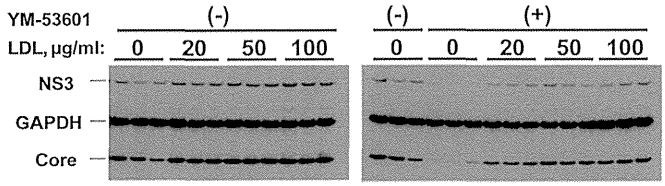

FIG 7 The anti-HCV effect of YM-53601 is significantly reversed by LDL. Huh-7.5.1-8 cells were infected with HCV JFH-1 and then treated with 1 μM YM-53601 or DMSO in serum-free medium that contained 0 to 100 μg/ml of LDL for 5 days. An equal portion of each cell lysate was subjected to immunoblotting for core, NS3, and GAPDH proteins. The results from one representative experiment performed in triplicates are shown. Similar results were obtained in two independent experiments.

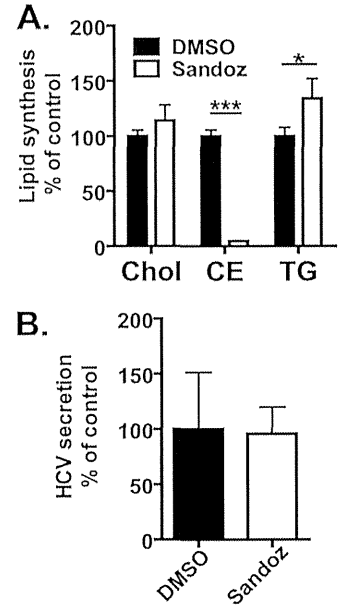

FIG 8 An ACAT inhibitor, Sandoz 58-035, does not exhibit an anti-HCV effect. (A) Huh-7.5.1-8 cells were pretreated with 30 μM Sandoz 58-035 or its vehicle, DMSO, in serum-free medium for 24 h. The cells were subsequently labeled using [^{3}H]acetate in the same medium as for the pretreatment for 18 h. The lipid fractions were extracted from cells and separated by TLC. The incorporation of [^{3}H]acetate into cholesterol (Chol), cholesteryl esters (CE), and triglycerides (TG) was quantified and expressed as a percentage of the control value. (B) Huh-7.5.1-8 cells were infected with HCV JFH-1 and then treated with Sandoz 58-035 or DMSO (control) under the same conditions as described above. The culture supernatants were harvested on the fifth day postinfection. The amount of secreted viral particles in each culture supernatant was determined by ELISA for the core protein and is expressed as a percentage of the control value. Data in each graph are means ± SD for triplicate samples from one representative experiment. Similar results were obtained in two independent experiments. *, $P < 0.05$; ***$P < 0.001$.

cholesterol content (Fig. 4D), raising the possibility that biosynthesis of cholesteryl esters is more important for HCV production than that of cholesterol. To test this possibility, we examined the effect of Sandoz 58-035, an inhibitor of acyl-CoA:cholesterol acyltransferase (ACAT) that catalyzes the biosynthesis of cholesteryl esters from cholesterol and fatty acyl-CoA, on HCV production. A metabolic labeling experiment with [^{3}H]acetate verified that treatment with 30 μM Sandoz 58-035 inhibits cholesteryl ester synthesis but not cholesterol and triglyceride syntheses in Huh-7.5.1-8 cells grown in serum-free medium (Fig. 8A). When Huh-7.5.1-8 cells were infected with HCV JFH-1 and then treated with either 30 μM Sandoz 58-035 or DMSO (control) in serum-free medium, virus secretion from the drug-treated cells was similar to that from the control cells (Fig. 8B). Taken together with the results shown in Fig. 3 and 4, these results suggest that biosynthesis of cholesterol, but not that of cholesteryl esters, is important for HCV production.

YM-53601 inhibits RNA replication of HCV JFH-1. To investigate which stages of the HCV life cycle are targeted by YM-53601, we conducted a transient-replication assay using a subgenomic replicon, SGR-JFH1/Luc (45). When cells are transfected with this replicon RNA, the self-encoded viral RNA replicase (NS3-NS5B) is expressed under the control of the EMCV IRES and then amplifies the replicon in the cells. The replicon also encodes luciferase translated under HCV IRES control, thereby allowing quantitation of viral RNA replication and translation activities via luciferase expression. Parallel transfection with a replication-incompetent mutant replicon, SGR-JFH1/Luc-GND (45), enables estimation of the level of replication-independent luciferase expression from the input replicon. As shown in Fig. 9A, luciferase activity in the wild-type replicon-transfected cells reached its peak at 47 h posttransfection and then declined. In the presence of YM-53601, the peak activity was decreased to approximately half of that in the control cells. The mutant replicon yielded very low luciferase activity irrespective of the drug treatment, confirming that the activity yielded by the wild-type replicon at 23 to 71 h posttransfection was dependent on viral RNA replication. Multiple experiments showed that the drug treatment lowered the peak luciferase activity to 52.6% ± 25.3% ($n = 5$; $P = 0.014$) of the control activity.

To test whether YM-53601 inhibits HCV IRES-dependent translation, we transfected drug-pretreated Huh-7.5.1-8 cells with the replication-incompetent mutant replicon SGR-JFH1/Luc-GND and then monitored luciferase expression in the presence of the drug for up to 21 h. Because the replicon cannot be replicated, luciferase activity yielded by the mutant replicon is attributable exclusively to HCV IRES-dependent translation and reflects the residual amount of the input replicon RNA. As shown in Fig. 9B, luciferase activity in the drug-treated cells and untreated control cells reached its peak at 3 h posttransfection and then declined. During the time course, the activity in the drug-treated cells was not lower, but rather was higher, than the activity in the control cells. Furthermore, the level of NS3 protein that was expressed from the mutant replicon changed similarly in the drug-treated and control cells, reaching its peak at 3 to 6 h posttransfection (Fig. 9C). Thus, it appears unlikely that YM-53601 impairs HCV IRES-dependent translation or viral RNA and NS protein stability.

Taken together, these results suggest that YM-53601 inhibits the RNA replication of HCV JFH-1.

YM-53601 does not affect the cellular distribution of NS4B protein. It is possible that YM-53601 alters the formation of the HCV-specific ultrastructure termed the membranous web, which serves as a scaffold for the viral RNA replication complex (55, 56), thereby inhibiting viral RNA replication. To test this possibility, we treated Huh-7.5.1-8 cells stably expressing HA-tagged NS4B protein with YM-53601 for 3 days in serum-free medium. It has been shown that the membranous web is induced by NS4B protein alone (55, 57) and appears as NS4B-accumulating foci or dots under fluorescence microscopy (58, 59). We found small intense foci that were detected with an anti-HA antibody in non-drug-

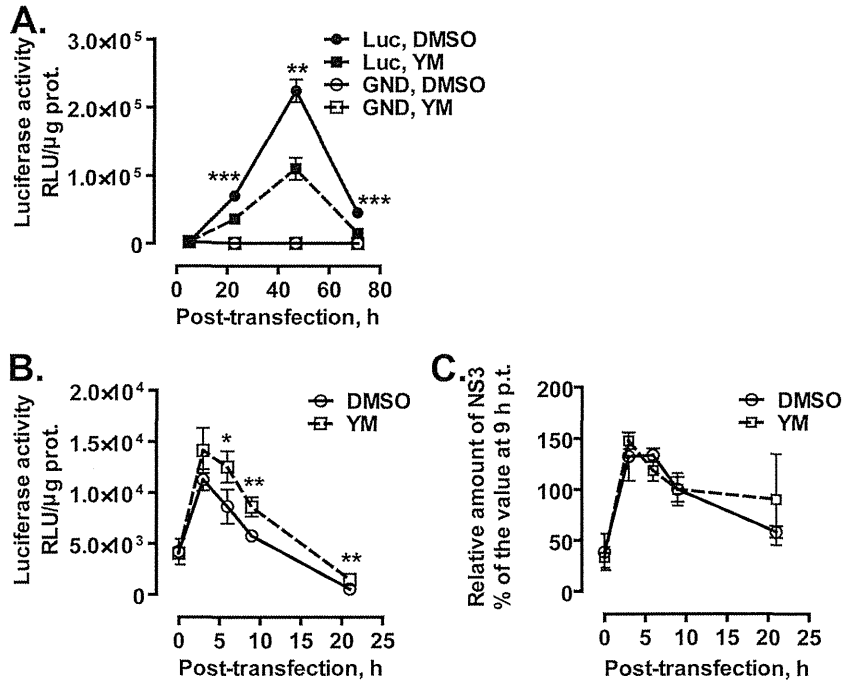

FIG 9 YM-53601 inhibits HCV RNA replication of HCV JFH-1. (A) Transient-replication assay using JFH-1 subgenomic replicons. Huh-7.5.1-8 cells were transfected with SGR-JFH1/Luc (closed symbols) or SGR-JFH1/Luc-GND (open symbols) RNAs by electroporation and then placed in serum-free medium. At 5 h posttransfection, YM-53601 (final concentration, 1.5 μM) (squares and dashed line) or DMSO (circles and solid line) was added to the medium. The cells were harvested at the indicated time points (posttransfection) and assayed for luciferase activity. (B and C) Huh-7.5.1-8 cells were pretreated with 1.5 μM YM-53601 or DMSO in serum-free medium for 42 h and then transfected with SGR-JFH1/Luc-GND RNA by lipofection. After transfection, the cells were further treated in the same medium and harvested at the indicated time points. (B) The cells were lysed and assayed for luciferase activity. (C) An equal amount of protein (10 μg/lane) in each cell lysate was subjected to immunoblotting for NS3 and GAPDH proteins, and each protein band was quantified. The relative amount of NS3 protein was calculated by dividing its intensity by that of GAPDH protein in the same lane. Data are expressed as a percentage of the relative amount at 9 h posttransfection. The value at 9 h posttransfection was not significantly different between the drug-treated and untreated cells (data not shown). Data in each graph are means ± SD for triplicate samples from one representative experiment. Similar results were obtained in at least two independent experiments. Statistical analysis was performed between drug-treated and control cells harboring the same replicon. *, $P < 0.05$; **$P < 0.01$; ***$P < 0.001$.

treated cells (Fig. 10C) and are similar to the NS4B foci previously reported (58, 60, 61). The foci were not detected in Huh-7.5.1-8 cells transfected with a backbone plasmid (Fig. 10A and B). Drug treatment resulted in no apparent alteration in NS4B foci (Fig. 10D) or the expression level of NS4B protein (data not shown), suggesting that the drug does not grossly alter the formation of the membranous web by NS4B protein.

RNA replication of HCV genotype 1b is not inhibited by YM-53601. To examine whether YM-53601 is able to inhibit viral RNA replication of HCV strains other than the JFH-1 strain (genotype 2a), we performed a transient-replication assay using a subgenomic replicon of the Con-1 strain (genotype 1b), FK-I_{389}Luci/NS3-3′/NK5.1 (46), and its replication-incompetent mutant, FK-I_{389}/Luci/NS3-3′/NK5.1/ΔGDD. Consistent with the previous report (46), time-dependent luciferase expression in the Con-1 replicon-transfected cells exhibited a downward-sloping pattern: luciferase activity at early time points (2.5 to 7 h posttransfection) was higher than the activity at later time points (Fig. 11A). At the early time points, the activity in the wild-type replicon-transfected cells was lower than the activity in the mutant replicon-transfected cells, indicating that RNA replication is too low to be detected at these early points. Afterwards, the activity in the wild-type replicon-transfected cells stayed higher than the activity in the mutant replicon-transfected cells, indicating that the difference between these activities was attributed to viral RNA replication. Unlike in the case of the JFH-1 replicon, treatment with YM-53601 did not lower RNA replication-dependent luciferase expression but rather enhanced it. From multiple experiments, the luciferase activity in the drug-treated cells at 46 to 50 h posttransfection was 284% ± 124% ($n = 4$) of the control activity.

To increase the impact of YM-53601, we performed a similar transient-replication assay using Huh-7.5.1-8 cells pretreated with the drug in serum-free medium for 2 days. Unexpectedly, serum-free preculture before transfection led to an overall decrease of two orders of magnitude in luciferase expression (Fig. 11B). In untreated control cells, RNA replication-dependent luciferase expression (i.e., the difference between the activity yielded by the wild-type replicon and that yielded by the mutant replicon) was not clearly found until 47 h posttransfection (compare black bars with hatched bars). However, RNA replication-dependent luciferase expression in drug-treated cells was found at and after 7 h posttransfection (compare gray bars with white bars) and was slightly higher than that in the untreated cells. Thus, the RNA replication-dependent luciferase expression does not appear to be inhibited by even a prolonged drug treatment.

Taken together, these results suggest that RNA replication of the Con-1 strain is not inhibited by YM-53601.

Entry of HCVpp of genotype 2a but not genotype 1b is blocked by YM-53601. To further investigate how YM-53601 blocks HCV production, we conducted an entry assay for HCV

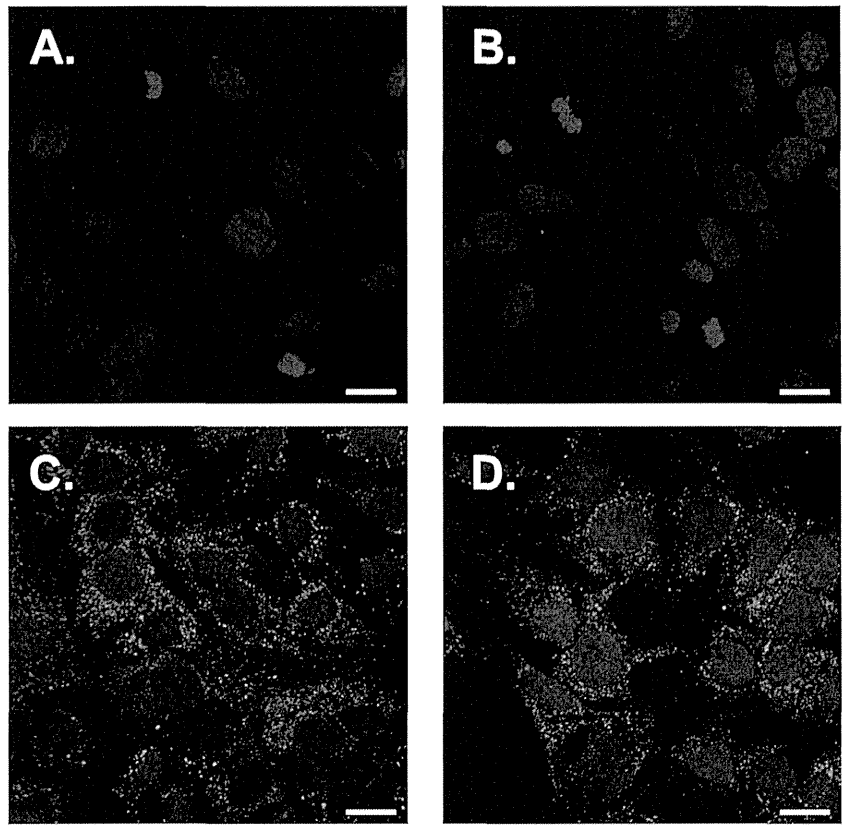

FIG 10 YM-53601 does not affect NS4B foci in Huh-7.5.1-8 cells. Huh-7.5.1-8 cells that were stably transfected with modified pCXN2 (A and B) or pCXN2/HA-TEV-NS4B (C and D) were grown on coverslips and treated with 1.5 μM YM-53601 (B and D) or DMSO (A and C) in serum-free medium for 3 days. The cells were fixed and subjected to immunofluorescence analysis using confocal microscopy. HA-tagged NS4B protein was detected with a rat anti-HA antibody followed by an Alexa Fluor 488-conjugated anti-rat antibody (green), and the nucleus was stained with DAPI (blue). Scale bars represent 20 μm.

pseudoparticles (HCVpp), which enter cells by using HCV envelope protein but replicate via a retroviral system (52). Although YM-53601 was added to cells after infection (Fig. 3 and 7), a block at the step of entry of progeny virus is possible because more than one round of infection can occur under our experimental conditions. Huh-7.5.1-8 cells were preincubated with YM-53601 in serum-free medium for 2 days and then infected in the presence of the drug with HCVpp harboring envelope glycoproteins from the JFH-1 strain. The cells were thereafter incubated in the absence of the drug for 3 days, and luciferase activity, reflecting the degree of HCVpp entry into host cells, was measured. Treatment with YM-53601 reduced luciferase activity to less than 50% of the activity in untreated cells (Fig. 12, left two bars). Infection with mock HCVpp prepared without envelope glycoproteins did not yield luciferase activity (<3 relative light units [RLU]/μg protein), confirming that luciferase expression is dependent on the envelope glycoproteins (data not shown). When the drug was added only at HCVpp infection, no reduction in the luciferase expression was found (Fig. 12, third bar from left), suggesting that the drug targets cells but not HCVpp. These results are consistent with the previous report showing partial cholesterol dependency of HCV entry (14). Similarly, we tested the effect of the drug on HCVpp harboring envelope glycoproteins from genotype 1b HCV (strain TH). Drug treatment before and during infection or only during infection did not significantly alter luciferase expression (Fig. 12, right three bars). Taken together, these results suggest that YM-53601 blocks entry of HCV genotype 2a but not that of genotype 1b.

DISCUSSION

The main aim of this study was to elucidate the importance of the committed pathway of cholesterol biosynthesis in the HCV life cycle. We have shown that three types of SQS inhibitor, YM-53601 (Fig. 3), zaragozic acid A (Fig. 5), and siSQS (Fig. 6), inhibited HCV JFH-1 production in Huh-7.5.1-8 cells in a similar manner. In particular, YM-53601 exerted an antiviral effect without remarkable cell toxicity. The antiviral effect of SQS inhibition was reversed by the addition of LDL (Fig. 6 and 7), indicating that the effect is attributable to cellular cholesterol and/or cholesteryl ester deficiencies (Fig. 4 and 6). Unlike YM-53601, no antiviral effect was observed with the ACAT inhibitor Sandoz 58-035 (Fig. 8), suggesting that synthesis of cholesterol rather than that of cholesteryl esters is important for HCV production. From these findings, we conclude that the committed pathway of cholesterol biosynthesis that begins with squalene synthesis (Fig. 1) plays an important role in the HCV life cycle. This conclusion is consistent with recent studies showing that inhibition of oxidosqualene cyclase, lanosterol C_{14}-demethylase, 24-dehydrocholesterol reductase, 7-dehydrocholesterol reductase, and SQS (discussed below) leads to decreased HCV production (31–33, 62). Furthermore, we propose that SQS is a potential target for anti-HCV strategies because all the SQS inhibitors tested in this study exerted anti-HCV effects.

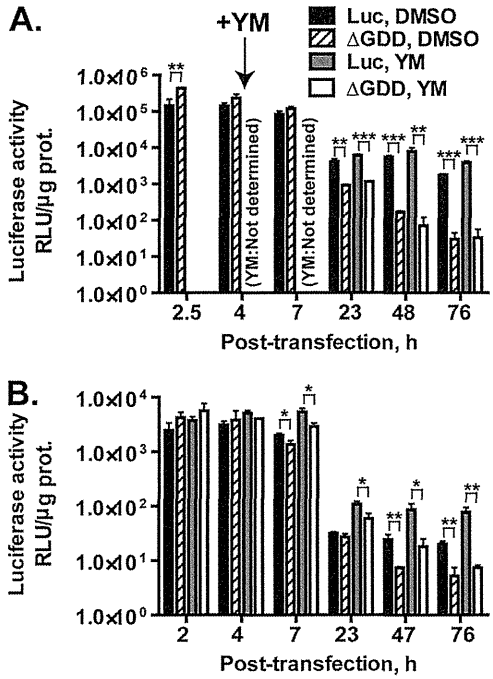

FIG 11 YM-53601 does not inhibit transient replication of Con-1 subgenomic replicons. (A) Huh-7.5.1-8 cells were transfected with FK-I_{389}Luci/NS3-3′/NK5.1 (Luc) (black and gray bars) or FK-I_{389}/Luci/NS3-3′/NK5.1/ΔGDD (ΔGDD) (hatched and white bars) RNAs by electroporation and then placed in serum-free medium. At 4 h posttransfection, YM-53601 (YM) (final concentration, 1.5 μM) (gray and white bars) or DMSO (black and hatched bars) was added to the medium. The cells were harvested at the indicated time points (posttransfection) and assayed for luciferase activity. (B) Huh-7.5.1-8 cells were pretreated with 1.5 μM YM-53601 or DMSO in serum-free medium for 47 h. The cells were transfected with FK-I_{389}Luci/NS3-3′/NK5.1 or FK-I_{389}/Luci/NS3-3′/NK5.1/ΔGDD RNAs and then further treated in the same medium. The cells were harvested at the indicated time points (posttransfection) and assayed for luciferase activity. Bars are as described for panel A. Data in each graph are means ± SD for triplicate samples from one representative experiment and are presented on a logarithmic scale because of large range of values. Some error bars are not visible due to their small sizes. Similar results were obtained in at least two independent experiments. *, $P < 0.05$; **$P < 0.01$; ***$P < 0.001$.

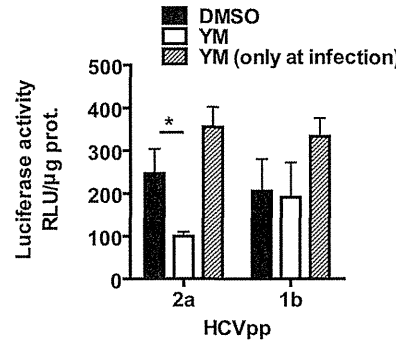

FIG 12 YM-53601 blocks entry of genotype 2a, but not genotype 1b, HCVpp. Huh-7.5.1-8 cells were grown in serum-free medium that contained 1.5 μM YM-53601 (white bars) or DMSO (black and hatched bars) for 2 days and then infected with HCVpp in the presence (white and hatched bars) or absence (black bars) of the drug. The cells were further grown in complete medium without the drug for 3 days and assayed for luciferase activity. Data are means ± SD for triplicate samples from one representative experiment. Similar results were obtained in two independent experiments. *, $P < 0.05$.

It has been reported that the peak plasma concentration of YM-53601 is 0.92 μg/ml (approximately 2.5 μM) after oral administration in rats at a dose with a cholesterol-lowering effect (38, 63). This concentration is roughly close to the IC_{50} of YM-53601 for HCV production in the presence of serum. Thus, YM-53601 might exert an anti-HCV effect *in vivo*.

Using a transient-replication assay (Fig. 9A) and the HCVpp system (Fig. 12), we found that suppression of HCV RNA replication and entry is involved in the antiviral mechanism of YM-53601 against JFH-1 virus. However, the degrees of suppression of these processes were at most approximately 50% in our assays. Accordingly, these mechanisms alone may not explain the more severe inhibition of HCV production observed in the HCV cell culture system (Fig. 3). Possibly, some steps in the HCV life cycle other than RNA replication and entry might be sensitive to the drug. Alternatively, some steps which are not reproduced in the subgenomic replicon and HCVpp systems might be more sensitive to the drug.

YM-53601 inhibited transient RNA replication of the subgenomic reporter replicon from the JFH-1 strain (genotype 2a) (Fig. 9A) but somewhat enhanced that of the subgenomic replicon from the Con-1 strain (genotype 1b) (Fig. 11). Similarly, the drug inhibited entry of genotype 2a, but not genotype 1b, HCVpp (Fig. 12). These findings raise the possibility that the cholesterol requirement for HCV RNA replication and entry varies among virus genotypes. Consistent with our results, previous studies have shown that SQS inhibition by zaragozic acid A leads to an enhancement of genotype 1b RNA replication (28, 31). This proviral effect appears to be caused by an increase in geranylgeranyl pyrophosphate, which is required for geranylgeranylation of a viral host factor and elevated expression of HMG-CoA reductase (31). In the case of genotype 2a, the proviral effect might be overwhelmed by antiviral effect caused by cholesterol depletion. Interestingly, genotype-specific inhibition of HCV RNA replication was also observed with inhibitors of sphingomyelin biosynthesis (19, 64, 65). Thus, major components of lipid rafts, i.e., cholesterol and sphingomyelin, appear to be similar in that they both contribute to HCV RNA replication in a genotype-dependent manner.

During preparation of this paper, Park et al. reported that siRNAs against farnesyl-diphosphate farnesyltransferase 1 (another name for SQS) and YM-53601 impair propagation of the HCV Jc1 strain (genotype 2a) in Huh-7.5 cells (62). They suggested that these agents target viral RNA replication by using a luciferase-encoding full genomic replicon of the JFH-1 strain and genotype 2a subgenomic replicon cells. These findings are consistent with our results. However, their finding that the viral RNA level in genotype 1b subgenomic replicon cells is decreased by SQS knockdown appears to argue against our results, as we could not find any antiviral effect of YM-53601 on genotype 1b RNA replication (Fig. 11). Although the reason for this discrepancy is currently unknown, differences in the culture conditions (serum-containing medium versus serum-free medium), replication assay (RT-qPCR versus reporter), methods of SQS inhibition (siRNA versus drug), and origin of the subgenomic replicon might be involved. In any case, we should evaluate the effects of SQS inhibitors on the complete life cycle of HCV genotype 1b when cell culture systems capable of supporting its growth are developed.

Our data suggest that biosynthesis of cholesterol, rather than that of cholesteryl esters, is important for HCV production (Fig. 8). Treatment with YM-53601 led to only a slight reduction in cholesterol levels (Fig. 4D) but severely impaired HCV production, implying that the drug selectively decreases relatively minor but specific pools of cellular cholesterol that are important for HCV production. Given that lipid rafts may serve as sites for viral RNA replication (15–17), assembly (19, 20), and virus entry (14, 19, 66), one scenario is that YM-53601 might selectively decrease lipid raft-associated cholesterol, thereby perturbing these processes. Consistent with this proposition, inhibition of SQS in prostate cancer cells results in a decrease of raft-associated cholesterol rather than nonraft cholesterol (67). On the other hand, a recent study has shown that purified double-membrane vesicles containing active HCV RNA replication complexes are highly enriched with cholesterol (68), although they originate from the ER, which is poor in cholesterol (69). It has also been shown that cholesterol depletion from the double-membrane vesicles decreases viral RNA levels associated with them, suggesting that cholesterol is an important structural component of HCV RNA replication complexes. Cholesterol biosynthesis (70) and HCV RNA replication (71, 72) both occur in the ER, and some cholesterol biosynthetic enzymes, including SQS, are partially copurified with components of HCV RNA replication complexes (73), implying that the cholesterol biosynthetic machinery might be closely associated with HCV RNA replication complexes in the ER. Thus, another scenario is that YM-53601 might decrease newly synthesized ER cholesterol pools, which might be preferentially used for structural components of membrane-bound viral RNA replication complexes. Preferential use of newly synthesized cholesterol in the formation of envelope membranes of human immunodeficiency virus has been found (74). Note that we could not detect any impact of YM-53601 on the morphology of NS4B-induced foci, which are considered scaffolds of viral RNA replication complexes, under fluorescence microscopy (Fig. 10). Thus, alteration in the structure of RNA replication complexes caused by YM-53601, if any, might be found at the ultrastructural level.

AQ: C

Our data provide evidence that the committed pathway of cholesterol biosynthesis is important for HCV production, consistent with recent studies (31–33, 62). Moreover, we found that biosynthesis of cholesterol, but not of cholesteryl esters, is important for this process. The identity of the cholesterol pools required for HCV production and the molecular mechanisms underlying the cholesterol requirement should be elucidated in future studies. Our data also provide concrete evidence that SQS is a potential anti-HCV target. Further studies are required to ascertain the anti-HCV activity of SQS inhibitors *in vivo*. SQS inhibitors are expected to exert fewer adverse effects on human cells than statins because SQS inhibitors lower cholesterol without depleting nonsterol isoprenoids (75, 76). For this reason, many compounds targeting SQS have been developed in the past by the pharmaceutical industry as potential cholesterol-lowering drugs for hypercholesterolemia. Thus, reevaluation of these compounds for potential anti-HCV activity might offer a time-saving and cost-effective approach for developing anti-HCV drugs.

ACKNOWLEDGMENTS

The pFK-I_{389}Luci/NS3-3′/NK5.1 and pFK-I_{389}neo/NS3-3′/NK5.1/ΔGDD plasmids were kind gifts from Ralf Bartenschlager. We thank Kiyoshi Kawasaki (Doshisha Woman's College) for useful suggestions and Toshiyuki Yamaji for technical assistance.

This study was supported by the National Cancer Center Research and Development Fund (grant no. 7 to M.F.) from the National Cancer Center of Japan, by Health and Labor Sciences research grants for research on hepatitis from the Ministry of Health, Labor and Welfare of Japan, and by Grants-in-Aid for Scientific Research (C) JSPS KAKENHI (grant no. 21590085 to K.S. and 23590104 to M.F.) from the Japan Society for the Promotion of Science.

REFERENCES

1. World Health Organization. 2014. Hepatitis C fact sheet no. 164. World Health Organization, Geneva, Switzerland. http://www.who.int/mediacentre/factsheets/fs164/en/.
2. Ghany MG, Strader DB, Thomas DL, Seeff LB. 2009. Diagnosis, management, and treatment of hepatitis C: an update. Hepatology 49:1335–1374. http://dx.doi.org/10.1002/hep.22759.
3. Alexopoulou A, Papatheodoridis GV. 2012. Current progress in the treatment of chronic hepatitis C. World J Gastroenterol 18:6060–6069. http://dx.doi.org/10.3748/wjg.v18.i42.6060.
4. Doyle JS, Aspinall E, Liew D, Thompson AJ, Hellard ME. 2013. Current and emerging antiviral treatments for hepatitis C infection. Br J Clin Pharmacol 75:931–943. http://dx.doi.org/10.1111/j.1365-2125.2012.04419.x.
5. Lawitz E, Sulkowski MS, Ghalib R, Rodriguez-Torres M, Younossi ZM, Corregidor A, DeJesus E, Pearlman B, Rabinovitz M, Gitlin N, Lim JK, Pockros PJ, Scott JD, Fevery B, Lambrecht T, Ouwerkerk-Mahadevan S, Callewaert K, Symonds WT, Picchio G, Lindsay KL, Beumont M, Jacobson IM. 2014. Simeprevir plus sofosbuvir, with or without ribavirin, to treat chronic infection with hepatitis C virus genotype 1 in non-responders to pegylated interferon and ribavirin and treatment-naive patients: the COSMOS randomised study. Lancet 384:1756–1765. http://dx.doi.org/10.1016/S0140-6736(14)61036-9.
6. Schneider MD, Sarrazin C. 2014. Antiviral therapy of hepatitis C in 2014: do we need resistance testing? Antiviral Res 105:64–71. http://dx.doi.org/10.1016/j.antiviral.2014.02.011.
7. Fraser CS, Doudna JA. 2007. Structural and mechanistic insights into hepatitis C viral translation initiation. Nat Rev Microbiol 5:29–38. http://dx.doi.org/10.1038/nrmicro1558.
8. Grakoui A, Wychowski C, Lin C, Feinstone SM, Rice CM. 1993. Expression and identification of hepatitis C virus polyprotein cleavage products. J Virol 67:1385–1395.
9. Bartenschlager R, Ahlborn-Laake L, Mous J, Jacobsen H. 1993. Nonstructural protein 3 of the hepatitis C virus encodes a serine-type proteinase required for cleavage at the NS3/4 and NS4/5 junctions. J Virol 67:3835–3844.
10. Hijikata M, Mizushima H, Tanji Y, Komoda Y, Hirowatari Y, Akagi T, Kato N, Kimura K, Shimotohno K. 1993. Proteolytic processing and membrane association of putative nonstructural proteins of hepatitis C virus. Proc Natl Acad Sci U S A 90:10773–10777. http://dx.doi.org/10.1073/pnas.90.22.10773.
11. Moradpour D, Penin F, Rice CM. 2007. Replication of hepatitis C virus. Nat Rev Microbiol 5:453–463. http://dx.doi.org/10.1038/nrmicro1645.
12. Moradpour D, Gosert R, Egger D, Penin F, Blum HE, Bienz K. 2003. Membrane association of hepatitis C virus nonstructural proteins and identification of the membrane alteration that harbors the viral replication complex. Antiviral Res 60:103–109. http://dx.doi.org/10.1016/j.antiviral.2003.08.017.
13. Felmlee DJ, Hafirassou ML, Lefevre M, Baumert TF, Schuster C. 2013. Hepatitis C virus, cholesterol and lipoproteins—impact for the viral life cycle and pathogenesis of liver disease. Viruses 5:1292–1324. http://dx.doi.org/10.3390/v5051292.
14. Kapadia SB, Barth H, Baumert T, McKeating JA, Chisari FV. 2007. Initiation of hepatitis C virus infection is dependent on cholesterol and cooperativity between CD81 and scavenger receptor B type I. J Virol 81:374–383. http://dx.doi.org/10.1128/JVI.01134-06.
15. Aizaki H, Lee KJ, Sung VM, Ishiko H, Lai MM. 2004. Characterization of the hepatitis C virus RNA replication complex associated with lipid rafts. Virology 324:450–461. http://dx.doi.org/10.1016/j.virol.2004.03.034.
16. Shi ST, Lee KJ, Aizaki H, Hwang SB, Lai MM. 2003. Hepatitis C virus RNA replication occurs on a detergent-resistant membrane that cofractionates with caveolin-2. J Virol 77:4160–4168. http://dx.doi.org/10.1128/JVI.77.7.4160-4168.2003.

17. Gao L, Aizaki H, He JW, Lai MM. 2004. Interactions between viral nonstructural proteins and host protein hVAP-33 mediate the formation of hepatitis C virus RNA replication complex on lipid raft. J Virol 78: 3480–3488. http://dx.doi.org/10.1128/JVI.78.7.3480-3488.2004.
18. Lingwood D, Simons K. 2010. Lipid rafts as a membrane-organizing principle. Science 327:46–50. http://dx.doi.org/10.1126/science.1174621.
19. Aizaki H, Morikawa K, Fukasawa M, Hara H, Inoue Y, Tani H, Saito K, Nishijima M, Hanada K, Matsuura Y, Lai MM, Miyamura T, Wakita T, Suzuki T. 2008. Critical role of virion-associated cholesterol and sphingolipid in hepatitis C virus infection. J Virol 82:5715–5724. http://dx.doi.org/10.1128/JVI.02530-07.
20. Matto M, Rice CM, Aroeti B, Glenn JS. 2004. Hepatitis C virus core protein associates with detergent-resistant membranes distinct from classical plasma membrane rafts. J Virol 78:12047–12053. http://dx.doi.org/10.1128/JVI.78.21.12047-12053.2004.
21. Miyanari Y, Atsuzawa K, Usuda N, Watashi K, Hishiki T, Zayas M, Bartenschlager R, Wakita T, Hijikata M, Shimotohno K. 2007. The lipid droplet is an important organelle for hepatitis C virus production. Nat Cell Biol 9:1089–1097. http://dx.doi.org/10.1038/ncb1631.
22. Bartenschlager R, Penin F, Lohmann V, Andre P. 2011. Assembly of infectious hepatitis C virus particles. Trends Microbiol 19:95–103. http://dx.doi.org/10.1016/j.tim.2010.11.005.
23. Hishiki T, Shimizu Y, Tobita R, Sugiyama K, Ogawa K, Funami K, Ohsaki Y, Fujimoto T, Takaku H, Wakita T, Baumert TF, Miyanari Y, Shimotohno K. 2010. Infectivity of hepatitis C virus is influenced by association with apolipoprotein E isoforms. J Virol 84:12048–12057. http://dx.doi.org/10.1128/JVI.01063-10.
24. Merz A, Long G, Hiet MS, Brugger B, Chlanda P, Andre P, Wieland F, Krijnse-Locker J, Bartenschlager R. 2011. Biochemical and morphological properties of hepatitis C virus particles and determination of their lipidome. J Biol Chem 286:3018–3032. http://dx.doi.org/10.1074/jbc.M110.175018.
25. Goldstein JL, Brown MS. 1990. Regulation of the mevalonate pathway. Nature 343:425–430. http://dx.doi.org/10.1038/343425a0.
26. Schachter M. 2005. Chemical, pharmacokinetic and pharmacodynamic properties of statins: an update. Fundam Clin Pharmacol 19:117–125. http://dx.doi.org/10.1111/j.1472-8206.2004.00299.x.
27. Ye J, Wang C, Sumpter R, Jr, Brown MS, Goldstein JL, Gale M, Jr. 2003. Disruption of hepatitis C virus RNA replication through inhibition of host protein geranylgeranylation. Proc Natl Acad Sci U S A 100:15865–15870. http://dx.doi.org/10.1073/pnas.2237238100.
28. Kapadia SB, Chisari FV. 2005. Hepatitis C virus RNA replication is regulated by host geranylgeranylation and fatty acids. Proc Natl Acad Sci U S A 102:2561–2566. http://dx.doi.org/10.1073/pnas.0409834102.
29. Ikeda M, Abe K, Yamada M, Dansako H, Naka K, Kato N. 2006. Different anti-HCV profiles of statins and their potential for combination therapy with interferon. Hepatology 44:117–125. http://dx.doi.org/10.1002/hep.21232.
30. Brautbar A, Ballantyne CM. 2011. Pharmacological strategies for lowering LDL cholesterol: statins and beyond. Nat Rev Cardiol 8:253–265. http://dx.doi.org/10.1038/nrcardio.2011.2.
31. Owens CM, Mawhinney C, Grenier JM, Altmeyer R, Lee MS, Borisy AA, Lehar J, Johansen LM. 2010. Chemical combinations elucidate pathway interactions and regulation relevant to hepatitis C replication. Mol Syst Biol 6:375.
32. Rodgers MA, Villareal VA, Schaefer EA, Peng LF, Corey KE, Chung RT, Yang PL. 2012. Lipid metabolite profiling identifies desmosterol metabolism as a new antiviral target for hepatitis C virus. J Am Chem Soc 134: 6896–6899. http://dx.doi.org/10.1021/ja207391q.
33. Takano T, Tsukiyama-Kohara K, Hayashi M, Hirata Y, Satoh M, Tokunaga Y, Tateno C, Hayashi Y, Hishima T, Funata N, Sudoh M, Kohara M. 2011. Augmentation of DHCR24 expression by hepatitis C virus infection facilitates viral replication in hepatocytes. J Hepatol 55: 512–521. http://dx.doi.org/10.1016/j.jhep.2010.12.011.
34. Tansey TR, Shechter I. 2000. Structure and regulation of mammalian squalene synthase. Biochim Biophys Acta 1529:49–62. http://dx.doi.org/10.1016/S1388-1981(00)00137-2.
35. Wakita T, Pietschmann T, Kato T, Date T, Miyamoto M, Zhao Z, Murthy K, Habermann A, Krausslich HG, Mizokami M, Bartenschlager R, Liang TJ. 2005. Production of infectious hepatitis C virus in tissue culture from a cloned viral genome. Nat Med 11:791–796. http://dx.doi.org/10.1038/nm1268.
36. Zhong J, Gastaminza P, Cheng G, Kapadia S, Kato T, Burton DR, Wieland SF, Uprichard SL, Wakita T, Chisari FV. 2005. Robust hepatitis C virus infection in vitro. Proc Natl Acad Sci U S A 102:9294–9299. http://dx.doi.org/10.1073/pnas.0503596102.
37. Shirasago Y, Sekizuka T, Saito K, Suzuki T, Wakita T, Hanada K, Kuroda M, Abe R, Fukasawa M. Isolation and characterization of a Huh.7.5.1-derived cell clone highly permissive to hepatitis C virus. Jpn J Infect Dis, in press. AQ: D
38. Ugawa T, Kakuta H, Moritani H, Matsuda K, Ishihara T, Yamaguchi M, Naganuma S, Iizumi Y, Shikama H. 2000. YM-53601, a novel squalene synthase inhibitor, reduces plasma cholesterol and triglyceride levels in several animal species. Br J Pharmacol 131:63–70. http://dx.doi.org/10.1038/sj.bjp.0703545.
39. Bergstrom JD, Kurtz MM, Rew DJ, Amend AM, Karkas JD, Bostedor RG, Bansal VS, Dufresne C, VanMiddlesworth FL, Hensens OD, Liesch JM, Zink DL, Wilson KE, Onishi J, Milligan JA, Bills G, Kaplan L, Nallin Omstead M, Jenkins RG, Huang L, Meinz MS, Quinn L, Burg RW, Kong YL, Mochales S, Mojena M, Martin I, Pelaez F, Diez MT, Alberts AW. 1993. Zaragozic acids: a family of fungal metabolites that are picomolar competitive inhibitors of squalene synthase. Proc Natl Acad Sci U S A 90:80–84. http://dx.doi.org/10.1073/pnas.90.1.80.
40. Ross AC, Go KJ, Heider JG, Rothblat GH. 1984. Selective inhibition of acyl coenzyme A:cholesterol acyltransferase by compound 58-035. J Biol Chem 259:815–819.
41. Hanada K, Nishijima M, Kiso M, Hasegawa A, Fujita S, Ogawa T, Akamatsu Y. 1992. Sphingolipids are essential for the growth of Chinese hamster ovary cells. Restoration of the growth of a mutant defective in sphingoid base biosynthesis by exogenous sphingolipids. J Biol Chem 267: 23527–23533.
42. Kato T, Matsumura T, Heller T, Saito S, Sapp RK, Murthy K, Wakita T, Liang TJ. 2007. Production of infectious hepatitis C virus of various genotypes in cell cultures. J Virol 81:4405–4411. http://dx.doi.org/10.1128/JVI.02334-06.
43. Bligh EG, Dyer WJ. 1959. A rapid method of total lipid extraction and purification. Can J Biochem Physiol 37:911–917. http://dx.doi.org/10.1139/o59-099.
44. Mizoguchi T, Edano T, Koshi T. 2004. A method of direct measurement for the enzymatic determination of cholesteryl esters. J Lipid Res 45:396–401. http://dx.doi.org/10.1194/jlr.D300024-JLR200.
45. Kato T, Date T, Miyamoto M, Sugiyama M, Tanaka Y, Orito E, Ohno T, Sugihara K, Hasegawa I, Fujiwara K, Ito K, Ozasa A, Mizokami M, Wakita T. 2005. Detection of anti-hepatitis C virus effects of interferon and ribavirin by a sensitive replicon system. J Clin Microbiol 43:5679–5684. http://dx.doi.org/10.1128/JCM.43.11.5679-5684.2005.
46. Krieger N, Lohmann V, Bartenschlager R. 2001. Enhancement of hepatitis C virus RNA replication by cell culture-adaptive mutations. J Virol 75:4614–4624. http://dx.doi.org/10.1128/JVI.75.10.4614-4624.2001.
47. Kato T, Date T, Miyamoto M, Furusaka A, Tokushige K, Mizokami M, Wakita T. 2003. Efficient replication of the genotype 2a hepatitis C virus subgenomic replicon. Gastroenterology 125:1808–1817. http://dx.doi.org/10.1053/j.gastro.2003.09.023.
48. Inoue Y, Murakami K, Hmwe SS, Aizaki H, Suzuki T. 2007. Transcriptomic comparison of human hepatoma Huh-7 cell clones with different hepatitis C virus replication efficiencies. Jpn J Infect Dis 60:173–178. AQ: E
49. Yamaji T, Nishikawa K, Hanada K. 2010. Transmembrane BAX inhibitor motif containing (TMBIM) family proteins perturbs a trans-Golgi network enzyme, Gb3 synthase, and reduces Gb3 biosynthesis. J Biol Chem 285:35505–35518. http://dx.doi.org/10.1074/jbc.M110.154229.
50. Niwa H, Yamamura K, Miyazaki J. 1991. Efficient selection for high-expression transfectants with a novel eukaryotic vector. Gene 108:193–199. http://dx.doi.org/10.1016/0378-1119(91)90434-D.
51. Yamaji T, Mitsuki M, Teranishi T, Hashimoto Y. 2005. Characterization of inhibitory signaling motifs of the natural killer cell receptor Siglec-7: attenuated recruitment of phosphatases by the receptor is attributed to two amino acids in the motifs. Glycobiology 15:667–676. http://dx.doi.org/10.1093/glycob/cwi048.
52. Bartosch B, Dubuisson J, Cosset FL. 2003. Infectious hepatitis C virus pseudo-particles containing functional E1-E2 envelope protein complexes. J Exp Med 197:633–642. http://dx.doi.org/10.1084/jem.20021756.
53. Murakami Y, Fukasawa M, Kaneko Y, Suzuki T, Wakita T, Fukazawa H. 2013. Selective estrogen receptor modulators inhibit hepatitis C virus infection at multiple steps of the virus life cycle. Microbes Infect 15:45–55. http://dx.doi.org/10.1016/j.micinf.2012.10.003.
54. Wakita T, Wands JR. 1994. Specific inhibition of hepatitis C virus ex-

pression by antisense oligodeoxynucleotides. In vitro model for selection of target sequence. J Biol Chem 269:14205–14210.
55. Egger D, Wolk B, Gosert R, Bianchi L, Blum HE, Moradpour D, Bienz K. 2002. Expression of hepatitis C virus proteins induces distinct membrane alterations including a candidate viral replication complex. J Virol 76:5974–5984. http://dx.doi.org/10.1128/JVI.76.12.5974-5984.2002.
56. Gosert R, Egger D, Lohmann V, Bartenschlager R, Blum HE, Bienz K, Moradpour D. 2003. Identification of the hepatitis C virus RNA replication complex in Huh-7 cells harboring subgenomic replicons. J Virol 77:5487–5492. http://dx.doi.org/10.1128/JVI.77.9.5487-5492.2003.
57. Konan KV, Giddings TH, Jr, Ikeda M, Li K, Lemon SM, Kirkegaard K. 2003. Nonstructural protein precursor NS4A/B from hepatitis C virus alters function and ultrastructure of host secretory apparatus. J Virol 77:7843–7855. http://dx.doi.org/10.1128/JVI.77.14.7843-7855.2003.
58. Lundin M, Monne M, Widell A, Von Heijne G, Persson MA. 2003. Topology of the membrane-associated hepatitis C virus protein NS4B. J Virol 77:5428–5438. http://dx.doi.org/10.1128/JVI.77.9.5428-5438.2003.
59. Gretton SN, Taylor AI, McLauchlan J. 2005. Mobility of the hepatitis C virus NS4B protein on the endoplasmic reticulum membrane and membrane-associated foci. J Gen Virol 86:1415–1421. http://dx.doi.org/10.1099/vir.0.80768-0.
60. Manna D, Aligo J, Xu C, Park WS, Koc H, Heo WD, Konan KV. 2010. Endocytic Rab proteins are required for hepatitis C virus replication complex formation. Virology 398:21–37. http://dx.doi.org/10.1016/j.virol.2009.11.034.
61. Han Q, Aligo J, Manna D, Belton K, Chintapalli SV, Hong Y, Patterson RL, van Rossum DB, Konan KV. 2011. Conserved GXXXG- and S/T-like motifs in the transmembrane domains of NS4B protein are required for hepatitis C virus replication. J Virol 85:6464–6479. http://dx.doi.org/10.1128/JVI.02298-10.
62. Park EM, Nguyen LN, Lim YS, Hwang SB. 2014. Farnesyl-diphosphate farnesyltransferase 1 regulates hepatitis C virus propagation. FEBS Lett 588:1813–1820. http://dx.doi.org/10.1016/j.febslet.2014.03.043.
63. Ishihara T, Kakuta H, Moritani H, Ugawa T, Sakamoto S, Tsukamoto S-I, Yanagisawa I. 2003. Syntheses of 3-ethylidenequinuclidine derivatives as squalene synthase inhibitors. 2. Enzyme inhibition and effects on plasma lipid levels. Bioorg Med Chem 11:3735–3745. http://dx.doi.org/10.1016/S0968-0896(03)00336-5.
64. Sakamoto H, Okamoto K, Aoki M, Kato H, Katsume A, Ohta A, Tsukuda T, Shimma N, Aoki Y, Arisawa M, Kohara M, Sudoh M. 2005. Host sphingolipid biosynthesis as a target for hepatitis C virus therapy. Nat Chem Biol 1:333–337. http://dx.doi.org/10.1038/nchembio742.
65. Weng L, Hirata Y, Arai M, Kohara M, Wakita T, Watashi K, Shimotohno K, He Y, Zhong J, Toyoda T. 2010. Sphingomyelin activates hepatitis C virus RNA polymerase in a genotype-specific manner. J Virol 84:11761–11770. http://dx.doi.org/10.1128/JVI.00638-10.
66. Voisset C, Lavie M, Helle F, Op De Beeck A, Bilheu A, Bertrand-Michel J, Terce F, Cocquerel L, Wychowski C, Vu-Dac N, Dubuisson J. 2008. Ceramide enrichment of the plasma membrane induces CD81 internalization and inhibits hepatitis C virus entry. Cell Microbiol 10:606–617. http://dx.doi.org/10.1111/j.1462-5822.2007.01070.x.
67. Brusselmans K, Timmermans L, Van de Sande T, Van Veldhoven PP, Guan G, Shechter I, Claessens F, Verhoeven G, Swinnen JV. 2007. Squalene synthase, a determinant of Raft-associated cholesterol and modulator of cancer cell proliferation. J Biol Chem 282:18777–18785. http://dx.doi.org/10.1074/jbc.M611763200.
68. Paul D, Hoppe S, Saher G, Krijnse-Locker J, Bartenschlager R. 2013. Morphological and biochemical characterization of the membranous hepatitis C virus replication compartment. J Virol 87:10612–10627. http://dx.doi.org/10.1128/JVI.01370-13.
69. Lange Y. 1991. Disposition of intracellular cholesterol in human fibroblasts. J Lipid Res 32:329–339.
70. Ikonen E. 2008. Cellular cholesterol trafficking and compartmentalization. Nat Rev Mol Cell Biol 9:125–138. http://dx.doi.org/10.1038/nrm2336.
71. Wolk B, Buchele B, Moradpour D, Rice CM. 2008. A dynamic view of hepatitis C virus replication complexes. J Virol 82:10519–10531. http://dx.doi.org/10.1128/JVI.00640-08.
72. Targett-Adams P, Boulant S, McLauchlan J. 2008. Visualization of double-stranded RNA in cells supporting hepatitis C virus RNA replication. J Virol 82:2182–2195. http://dx.doi.org/10.1128/JVI.01565-07.
73. Huang H, Sun F, Owen DM, Li W, Chen Y, Gale M, Jr, Ye J. 2007. Hepatitis C virus production by human hepatocytes dependent on assembly and secretion of very low-density lipoproteins. Proc Natl Acad Sci U S A 104:5848–5853. http://dx.doi.org/10.1073/pnas.0700760104.
74. Zheng YH, Plemenitas A, Fielding CJ, Peterlin BM. 2003. Nef increases the synthesis of and transports cholesterol to lipid rafts and HIV-1 progeny virions. Proc Natl Acad Sci U S A 100:8460–8465. http://dx.doi.org/10.1073/pnas.1437453100.
75. Charlton-Menys V, Durrington PN. 2008. Human cholesterol metabolism and therapeutic molecules. Exp Physiol 93:27–42. http://dx.doi.org/10.1113/expphysiol.2007.035147.
76. Trapani L, Segatto M, Ascenzi P, Pallottini V. 2011. Potential role of nonstatin cholesterol lowering agents. IUBMB Life 63:964–971. http://dx.doi.org/10.1002/iub.522.

Journal of General Virology (2014), 95, 2658–2667 DOI 10.1099/vir.0.068528-0

Alternative endocytosis pathway for productive entry of hepatitis C virus

Mami Matsuda,[1] Ryosuke Suzuki,[1] Chikako Kataoka,[1] Koichi Watashi,[1] Hideki Aizaki,[1] Nobuyuki Kato,[2] Yoshiharu Matsuura,[3] Tetsuro Suzuki[4] and Takaji Wakita[1]

Correspondence
Ryosuke Suzuki
ryosuke@niid.go.jp

[1]Department of Virology II, National Institute of Infectious Diseases, Tokyo, Japan

[2]Department of Tumor Virology, Okayama University Graduate School of Medicine, Dentistry, and Pharmaceutical Sciences, Okayama, Japan

[3]Research Institute for Microbial Diseases, Osaka University, Osaka, Japan

[4]Department of Infectious Diseases, Hamamatsu University School of Medicine, Shizuoka, Japan

Previous studies have shown that hepatitis C virus (HCV) enters human hepatic cells through interaction with a series of cellular receptors, followed by clathrin-mediated, pH-dependent endocytosis. Here, we investigated the mechanisms of HCV entry into multiple HCV-permissive human hepatocyte-derived cells using trans-complemented HCV particles (HCVtcp). Knockdown of CD81 and claudin-1, or treatment with bafilomycin A1, reduced infection in Huh-7 and Huh7.5.1 cells, suggesting that HCV entered both cell types via receptor-mediated, pH-dependent endocytosis. Interestingly, knockdown of the clathrin heavy chain or dynamin-2 (Dyn2), as well as expression of the dominant-negative form of Dyn2, reduced infection of Huh-7 cells with HCVtcp, whereas infectious entry of HCVtcp into Huh7.5.1 cells was not impaired. Infection of Huh7.5.1 cells with culture-derived HCV (HCVcc) via a clathrin-independent pathway was also observed. Knockdown of caveolin-1, ADP-ribosylation factor 6 (Arf6), flotillin, p21-activated kinase 1 (PAK1) and the PAK1 effector C-terminal binding protein 1 of E1A had no inhibitory effects on HCVtcp infection into Huh7.5.1 cells, thus suggesting that the infectious entry pathway of HCV into Huh7.5.1 cells was not caveolae-mediated, or Arf6- and flotillin-mediated endocytosis and macropinocytosis, but rather may have occurred via an undefined endocytic pathway. Further analysis revealed that HCV entry was clathrin- and dynamin-dependent in ORL8c and HepCD81/miR122 cells, but productive entry of HCV was clathrin- and dynamin-independent in Hep3B/miR122 cells. Collectively, these data indicated that HCV entered different target cells through different entry routes.

Received 29 May 2014
Accepted 1 August 2014

INTRODUCTION

Over 170 million people worldwide are chronically infected with hepatitis C virus (HCV), and are at risk of developing chronic hepatitis, cirrhosis and hepatocellular carcinoma (Hoofnagle, 2002). HCV is an enveloped virus belonging to the family *Flaviviridae*. Its genome is an uncapped 9.6 kb positive-stranded RNA consisting of the 5′-UTR, an ORF encoding viral proteins and the 3′-UTR (Suzuki *et al.*, 2007). A precursor polyprotein is further processed into structural proteins (core, E1, and E2), followed by p7 and non-structural (NS) proteins (NS2, NS3, NS4A, NS4B, NS5A and NS5B), by cellular and viral proteases.

Two supplementary figures are available with the online version of this paper.

Host–virus interactions are required during the initial steps of viral infection. Viruses enter the cells by various pathways, such as receptor-mediated endocytosis followed by pH-dependent or -independent fusion from endocytic compartments, or pH-independent fusion at the plasma membrane coupled with receptor-mediated signalling and coordinated disassembly of the actin cortex (Grove & Marsh, 2011). It was reported previously that CD81 (Bartosch *et al.*, 2003; McKeating *et al.*, 2004; Pileri *et al.*, 1998), scavenger receptor class B type I (SR-BI) (Bartosch *et al.*, 2003; Scarselli *et al.*, 2002), claudin-1 (Evans *et al.*, 2007; Liu *et al.*, 2009) and occludin (Benedicto *et al.*, 2009; Liu *et al.*, 2009; Ploss *et al.*, 2009) are critical molecules for HCV entry into cells. Recently, epidermal growth factor receptor and ephrin receptor type A2 were also identified as host cofactors for HCV entry, possibly by modulating interactions between CD81 and claudin-1 (Lupberger *et al.*,

2011). In addition, Niemann–Pick C1-like 1 (NPC1L1) cholesterol absorption receptor has been shown to play a role in HCV entry, probably at the fusion step (Sainz *et al.*, 2012).

Following receptor binding, HCV has been reported to enter cultured cells via clathrin-mediated endocytosis, the most common and best-characterized mode of endocytosis, following membrane fusion in early endosomes (Blanchard *et al.*, 2006; Codran *et al.*, 2006; Coller *et al.*, 2009; Meertens *et al.*, 2006; Trotard *et al.*, 2009) using retrovirus-based HCV pseudoparticles (HCVpp) and cell culture-produced HCV (HCVcc). Early steps in HCV infection, including the role of HCV glycoprotein heterodimers, receptor binding, internalization and pH-dependent endosomal fusion, have been at least in part mimicked by HCVpp. However, as HCVpp are generated in non-hepatic cells such as human embryo kidney 293T cells, it is likely that the cell-derived component(s) of HCVpp differ from those of HCVcc.

In the present study, we readdressed the HCV endocytosis pathway using trans-complemented HCV particles (HCVtcp) (Suzuki *et al.*, 2012), of which the packaged genome is a subgenomic replicon. HCVtcp, generated in Huh-7 or its derivative cell lines with two plasmids, are infectious, but support only single-round infection, thereby allowing us to examine infectious viral entry without the influence of reinfection. In addition, HCVtcp is useful for quantifying productive infection by measuring luciferase activity. Furthermore, it has been shown that the HCVtcp system is more relevant as a model of HCV infection than HCVpp (Suzuki *et al.*, 2012). Our results demonstrated conclusively that, in addition to the clathrin-mediated endocytosis pathway, HCV was capable of utilizing the clathrin- and dynamin-independent pathways for infectious entry of HCV into human liver-derived cells.

RESULTS

HCV entry depends on receptor-mediated, pH-dependent endocytosis

HCV has been shown to enter permissive cells through clathrin-mediated endocytosis and low pH-dependent fusion with endosomes mostly using HCVpp (Codran *et al.*, 2006; Meertens *et al.*, 2006; Trotard *et al.*, 2009), although some researchers have used HCVcc with limited cell lines (Blanchard *et al.*, 2006; Coller *et al.*, 2009). However, several distinct characteristics between HCVpp and HCVcc have recently been revealed with regard to morphogenesis and entry steps (Helle *et al.*, 2010; Sainz *et al.*, 2012; Suzuki *et al.*, 2012; Vieyres *et al.*, 2010). Therefore, in this study, we used HCVtcp, which exhibit similar characteristics to HCVcc when compared with HCVpp and support single-round infection (Suzuki *et al.*, 2012).

Initially, to determine whether receptor candidates such as CD81, claudin-1, occludin and SR-BI are essential for HCV entry into Huh-7 and Huh7.5.1 cells, we examined the knockdown effect of these molecules on HCVtcp infection. Knockdown of these receptors was confirmed by immunoblotting (Fig. 1a) and FACS analysis (Fig. 1b). It should be noted that the luciferase activity in Huh7.5.1 was approximately four times higher than that in Huh-7 cells when the same amount of inoculum was used for infection (Fig. S1, available in the online Supplementary Material), and knockdown did not affect cell viability (data not shown). Knockdown of CD81 and claudin-1 significantly reduced the infection of Huh-7 and Huh7.5.1 cells with HCVtcp derived from genotype 2a (Fig. 1c). Knockdown of occludin led to a moderate reduction in infection; however, only a marginal effect was observed in SR-BI knockdown in both Huh-7 and Huh7.5.1 cells (Fig. 1c), possibly due to the reduced requirement for SR-BI during virus entry by adaptive mutation in E2 (Grove *et al.*, 2008).

Next, to examine whether HCV entry was pH-dependent, Huh-7 and Huh7.5.1 cells were pretreated with bafilomycin A1, an inhibitor of vacuolar H^+-ATPases that impairs vesicle acidification, and then infected with HCVtcp. At 72 h post-infection, luciferase activity and cell viability were determined. Bafilomycin A1 inhibited HCVtcp infection in a dose-dependent manner without affecting cell viability in both Huh-7 and Huh7.5.1 cells (Fig. 2a, b). We also confirmed that treatment with bafilomycin A1 after HCVtcp infection had a minor effect on luciferase activity (Fig. 2c). These results indicated that the infectious route of HCVtcp into Huh-7 and Huh7.5.1 cells is receptor-mediated and involves pH-dependent endocytosis.

Knockdown of clathrin heavy chain (CHC) or dynamin-2 (Dyn2) reduces HCVtcp infection in Huh-7 cells, but not in Huh7.5.1 cells

Among the known pathways of pH-dependent viral endocytosis, clathrin-mediated dynamin-dependent endocytosis is a major endocytosis pathway. Chlorpromazine, an inhibitor of clathrin-dependent endocytosis, has been commonly used to study clathrin-mediated endocytosis; however, it exerts multiple side-effects on cell function as it targets numerous receptors and intracellular enzymes, and alters plasma membrane characteristics (Sieczkarski & Whittaker, 2002a). Therefore, we examined the HCV endocytosis pathway by knockdown of specific molecules required for the endocytosis pathway. CHC, a major structural protein in clathrin-coated vesicles, and Dyn2, a GTPase essential for clathrin-coated-pit scission from the plasma membrane, play important roles in the clathrin-mediated pathway. Another well-studied model of viral entry is caveolin-mediated endocytosis. The role of dynamin in both clathrin-mediated endocytosis and caveolae-dependent endocytosis has been established (Marsh & Helenius, 2006; Miaczynska & Stenmark, 2008). To examine the endocytosis pathways of HCV, small interfering RNAs (siRNAs) for CHC, Dyn2 and caveolin-1 (Cav1), or scrambled control siRNA, were transfected into Huh-7 or

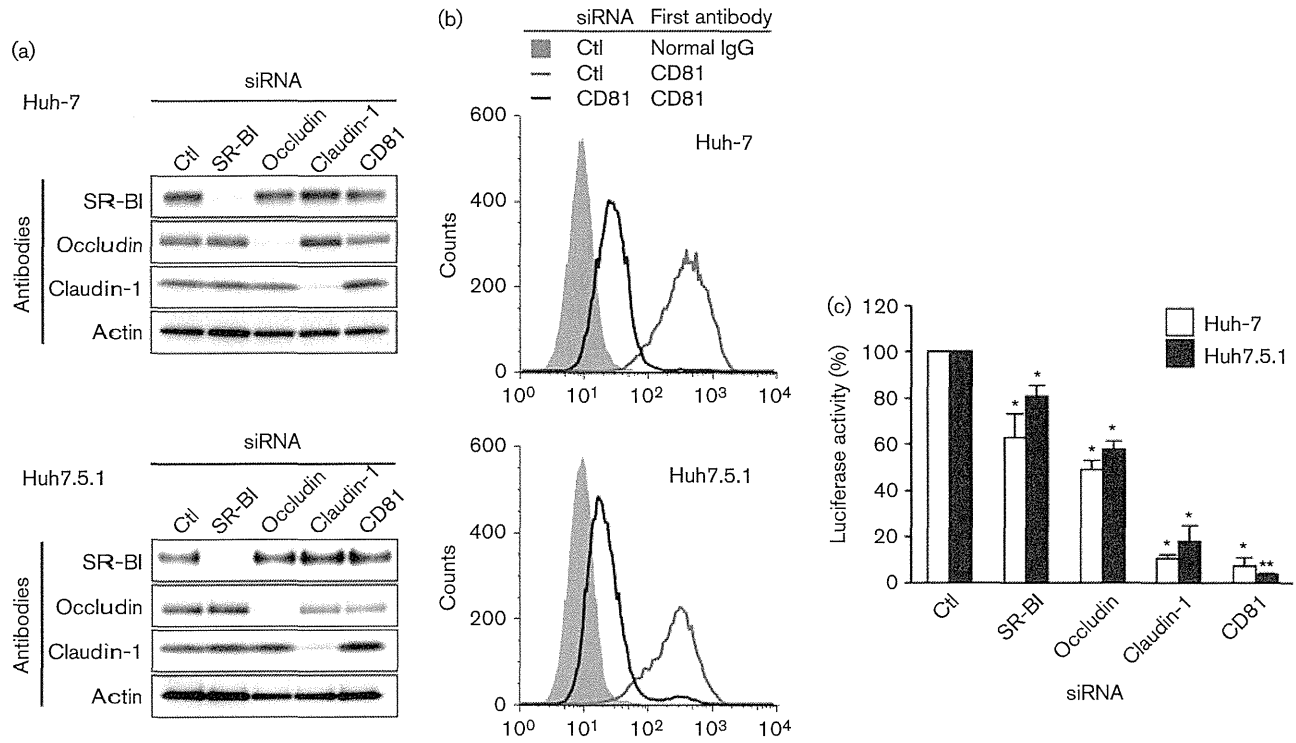

Fig. 1. Knockdown effect of receptor candidate molecules on HCV infection. (a) Huh-7 or Huh7.5.1 cells were transfected with the indicated small interfering RNAs (siRNA), harvested at 48 h post-transfection and the specific knockdown of each protein was verified by immunoblotting. (b) Huh-7 or Huh7.5.1 cells were transfected with CD81 or control siRNAs, harvested at 48 h post-transfection and the cell surface expression of CD81 was verified by FACS analysis. (c) Cells transfected with siRNA were infected with the same amount of HCVtcp at 48 h post-transfection. Firefly luciferase activity in the cells was determined at 72 h post-infection and is expressed relative to the activity with control siRNA transfection. The value for control (Ctl) siRNA was set at 100 %. Data represent the mean ± SD. Statistical differences between controls and each siRNA were evaluated using Student's *t*-test. **P*<0.05, ***P*<0.001 versus control.

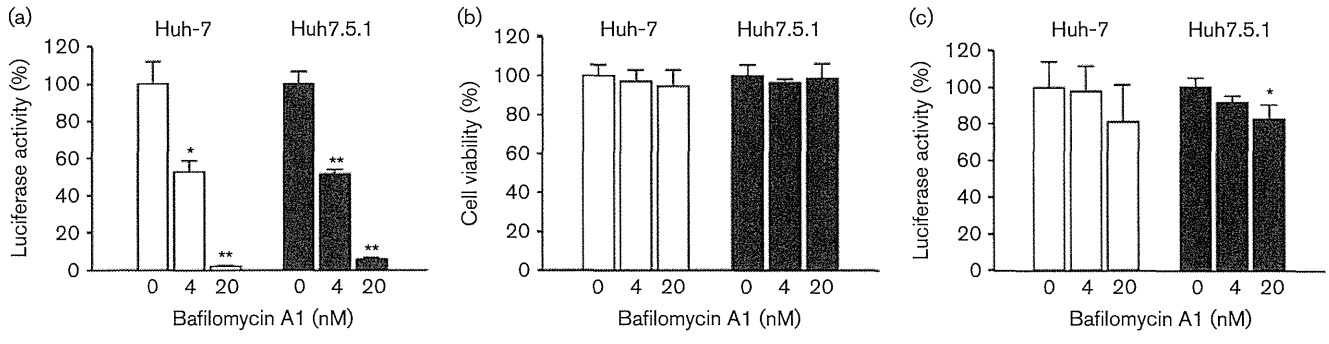

Fig. 2. Role of endosomal low pH in HCV infection. Cells were treated with bafilomycin A1 for 1 h at the indicated concentrations and infected with HCVtcp. (a, b) Luciferase activity (a) and cell viability (b) were determined at 72 h post-infection, and expressed relative to amounts observed in controls. (c) Cells were treated with bafilomycin A1 for 1 h at the indicated concentrations 48 h after HCVtcp infection. Luciferase activity was determined at 10 h post-treatment and expressed relative to amounts observed in controls. Data represent the mean ± SD. Statistical differences between controls and indicated concentrations were evaluated using Student's *t*-test. **P*<0.05, ***P*<0.001 versus control.

Huh7.5.1 cells, followed by infection with HCVtcp. Expression of CHC, Dyn2 and Cav1 was downregulated by transfection of specific siRNAs (Fig. 3a, b), whereas expression of SR-BI, occludin, claudin-1 and CD81 was not reduced (Figs 3a and S2). As indicated in Fig. 3(c), luciferase activity from HCVtcp was significantly reduced by knockdown of CHC and Dyn2 in Huh-7 cells, but not in Huh7.5.1 cells. Knockdown of Cav1 showed no inhibitory effects on HCVtcp entry into either cell line. Dynamin-independent entry in Huh7.5.1 cells was also observed using HCVtcp derived from genotype 1b (data not shown). Knockdown of CHC or Dyn2 also reduced entry of HCVcc in Huh-7 cells, but had no inhibitory effects in Huh7.5.1 (Fig. 3d). To rule out the possibility of effects on CHC and Dyn2 knockdown on viral RNA replication, HCVtcp were also inoculated before siRNA transfection. Luciferase activity was not affected by knockdown of CHC or Dyn2 in either cell line, whereas marked inhibition was observed for phosphatidylinositol 4-kinase (PI4K) (Fig. 3e). These data suggested that HCV entry was clathrin-mediated and dynamin-dependent in Huh-7 cells, but productive entry of HCV was clathrin- and dynamin-independent in Huh7.5.1 cells.

Expression of the dominant-negative form of Dyn2 reduces HCV infection in Huh-7 cells, but not in Huh7.5.1 cells

We also examined the role of dynamin in infectious entry of HCV into Huh-7 and Huh7.5.1 cells by overexpression of the dominant-negative form of Dyn2 (Dyn-K44A), which

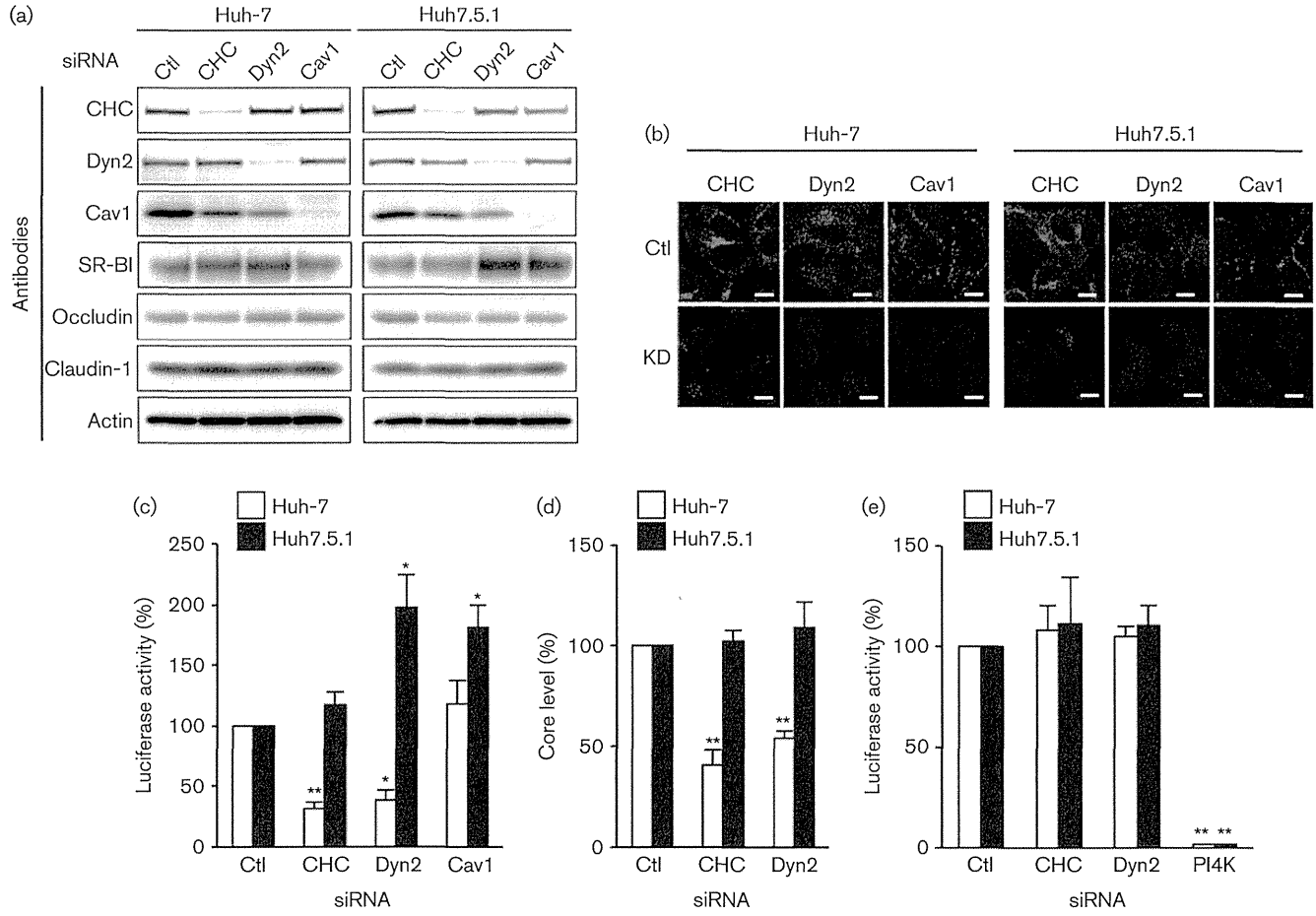

Fig. 3. Effects of CHC, Dyn2 and Cav1 knockdown on HCV infection. (a, b) Huh-7 cells or Huh7.5.1 cells were transfected with the indicated siRNAs and the specific knockdown (KD) of each protein was verified by immunoblotting (a) or immunostaining (b) at 48 h post-transfection. Bar, 50 μm. (c) Cells were transfected with the indicated siRNAs, followed by infection with HCVtcp at 48 h post-transfection. Firefly luciferase activity in the cells was subsequently determined at 3 days post-infection. The value for control (Ctl) siRNA was set at 100 %. Data represent the mean ± SD. (d) Cells were transfected with siRNA, followed by infection with HCVcc at 48 h post-transfection. Intracellular core levels were quantified at 24 h post-infection. The value for control siRNA was set at 100 %. Data represent the mean ± SD. (e) Cells were infected with HCVtcp, followed by transfection with the indicated siRNAs. Luciferase activity in the cells was subsequently determined at 2 days post-transfection. The value for control siRNA was set at 100 %. Data represent the mean ± SD. Statistical differences between controls and each siRNA were evaluated using Student's *t*-test. **P*<0.05, ***P*<0.001 versus control.

has been shown to effectively block clathrin-dependent and caveolar endocytosis (Damke *et al.*, 1995). Expression of haemagglutinin (HA)-tagged Dyn-K44A reduced the number of HCV-infected Huh-7 cells, but not Huh7.5.1 cells, as compared with WT HA-tagged Dyn2 (Dyn-WT), as shown in Fig. 4(a, b). Interestingly, internalization of transferrin, which is known to be mediated by clathrin-dependent endocytosis, was reduced in both Huh-7 and Huh7.5.1 cells expressing Dyn-K44A, whereas cells expressing Dyn-WT showed efficient endocytosis of transferrin (Fig. 4c, d). Collectively, these results suggested that dynamin participated in the internalization of HCV in Huh-7 cells, but was not absolutely required in Huh7.5.1 cells, although transferrin was taken up via dynamin-dependent endocytosis in both Huh-7 and Huh7.5.1 cells.

Flotillin-1 or the GTPase regulator associated with focal adhesion kinase 1 (GRAF1) play no major role during HCV infection of Huh7.5.1 cells

In order to dissect the major endocytosis pathways of HCVtcp in Huh7.5.1 cells, we investigated the role of alternative routes of HCV entry by siRNA knockdown. We silenced essential factors for the clathrin- or dynamin-independent pathways

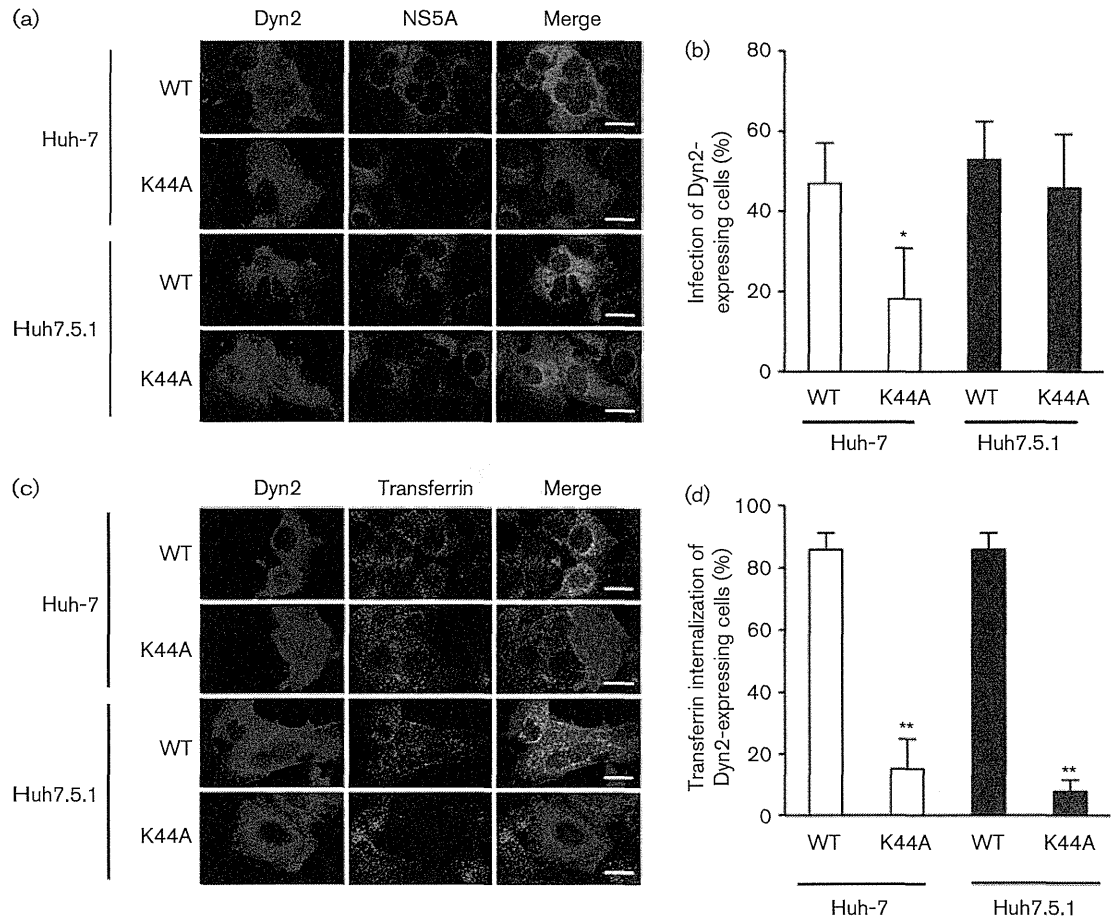

Fig. 4. Dynamin participates in the internalization of HCV in Huh-7 cells, but not in Huh7.5.1 cells. (a) Cells were transfected with HA-tagged WT Dyn2 (Dyn-WT) or dominant-negative Dyn2 (Dyn-K44A) expression plasmids. At 2 days post-transfection, cells were infected with HCVtcp, which possessed a subgenomic replicon without the luciferase gene. After 3 days, cells were fixed and HA-Dyn2 or HCV NS5A stained with anti-HA or anti-NS5A antibodies, respectively. Cell nuclei were counterstained with DAPI. Bar, 100 μm. (b) Data were quantified as the population of HCVtcp-infected cells among HA-positive cells. At least 20 HA-positive cells were evaluated in triplicate experiments. Data represent the mean ± SD. (c) Cells were transfected with HA-tagged Dyn-WT or Dyn-K44A expression plasmids. At 2 days post-transfection, cells were incubated with Alexa Fluor-488 labelled transferrin at 37 °C in a 5 % CO_2 incubator. After 30 min of incubation, cells were washed, fixed and stained with anti-HA antibodies. Cell nuclei were counterstained with DAPI. Bar, 100 μm. (d) Data were quantified as the population of transferrin-internalized cells among HA-positive cells. At least 20 HA-positive cells were evaluated in triplicate experiments. Data represent the mean ± SD. Statistical differences between Dyn-WT and Dyn-K44A were evaluated using Student's *t*-test. **P*<0.05, ***P*<0.001 versus Dyn-WT.

including flotillin-dependent endocytosis, ADP-ribosylation factor 6 (Arf6)-dependent endocytosis, clathrin-independent carrier/glycosylphosphatidylinositol-enriched early endosomal compartment (CLIC/GEEC) endocytic pathway and macropinocytosis in Huh7.5.1 cells. Flotillin-1 and Arf6 are indispensable components of the flotillin and Arf6 pathways, respectively. Knockdown of flotillin-1 or Arf6 had no inhibitory effects on HCVtcp infection in Huh7.5.1 cells (Fig. 5a). The CLIC/GEEC endocytic pathway has recently become better defined and is regulated by the GTPase regulator associated with focal adhesion kinase-1 (GRAF1). However, GRAF1 was not detected in Huh-7 or Huh7.5.1 cells (Fig. 5b); thus, it is unlikely that the CLIC/GEEC pathway was involved in HCV entry in Huh7.5.1 cells. In addition, knockdown of p21-activated kinase 1 (PAK1) and the PAK1 effector C-terminal binding protein 1 of E1A (CtBP1), which play important regulatory roles in the process of macropinocytosis, did not inhibit HCVtcp infection in Huh7.5.1 cells (Fig. 5c). Taken together, these results suggested that the entry of HCVtcp into Huh7.5.1 cells was not mediated mainly by flotillin-dependent endocytosis, Arf6-dependent endocytosis, the CLIC/GEEC endocytic pathway and macropinocytosis.

Clathrin-dependent and -independent pathways for HCV entry in other hepatic cells

We further examined the endocytosis pathways for HCV in non-Huh-7-related human liver-derived cell lines. Three HCVcc permissive hepatocellular carcinoma cell lines, Li23-derived ORL8c (Kato *et al.*, 2009), HepCD81/miR122 cells (HepG2/CD81 cells overexpressing miR122) and Hep3B/miR122 (Kambara *et al.*, 2012), were transfected with siRNA for CHC, Dyn2 or claudin-1, followed by infection with HCVtcp. Immunoblotting was performed in order to confirm knockdown of target proteins (Fig. 6a). Although knockdown of CHC or Dyn2 expression inhibited HCVtcp infection of ORL8c and HepCD81/miR122 cells, HCVtcp infection of Hep3B/miR122 cells was not affected (Fig. 6b), thus suggesting that productive entry of HCV is clathrin- and dynamin-independent in Hep3B/miR122 cells.

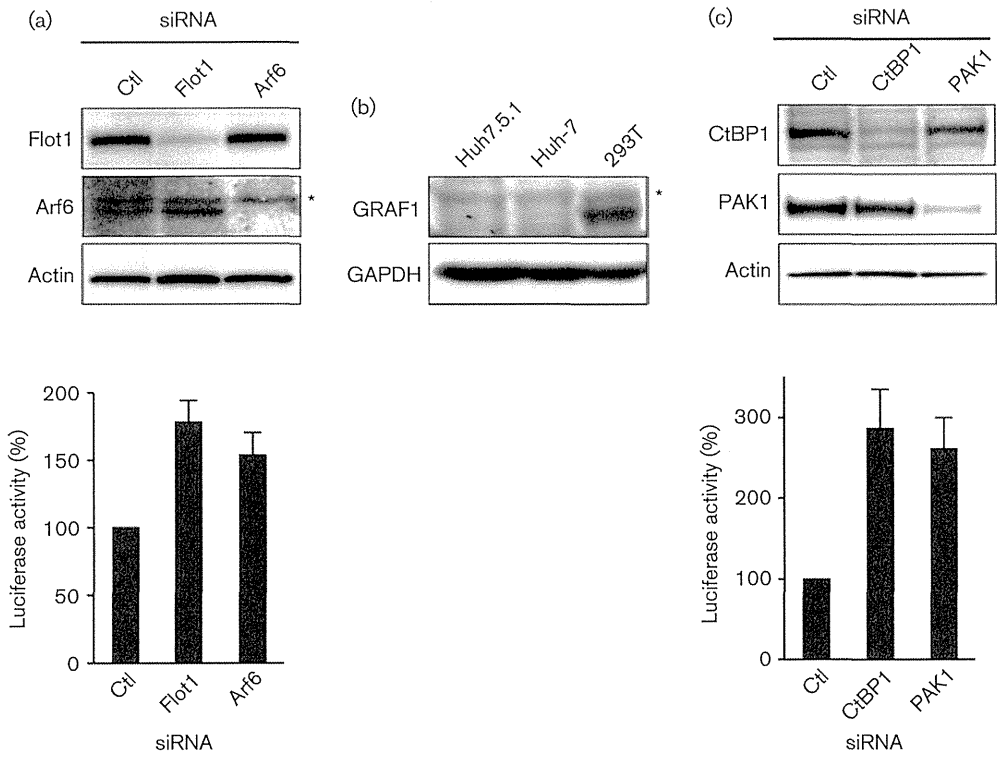

Fig. 5. Role of an alternative endocytosis pathway of HCV in Huh7.5.1 cells. (a) Huh7.5.1 cells were transfected with flotillin-1 (Flot1) or Arf6 siRNAs and specific knockdown of each protein was verified by immunoblotting (upper). Non-specific bands are marked with an asterisk. Cells transfected with siRNA were infected with HCVtcp. Luciferase activity (lower) was determined at 72 h post-infection and expressed relative to the amount observed in control (Ctl) siRNA transfection, Data represent the mean ± SD. (b) Expression of GRAF1 and glyceraldehyde 3-phosphate dehydrogenase (GAPDH) in Huh7.5.1, Huh-7 and 293T cells was analysed by immunoblotting. Non-specific bands are marked with an asterisk. (c) Huh7.5.1 cells were transfected with CtBP1 or PAK1 siRNA and specific knockdown of each protein was verified by immunoblotting (upper). Cells transfected with siRNA were infected with the HCVtcp. Luciferase activity (lower) was determined at 72 h post-infection and expressed relative to the amount observed in control (Ctl) siRNA transfection. Data represent the mean ± SD.

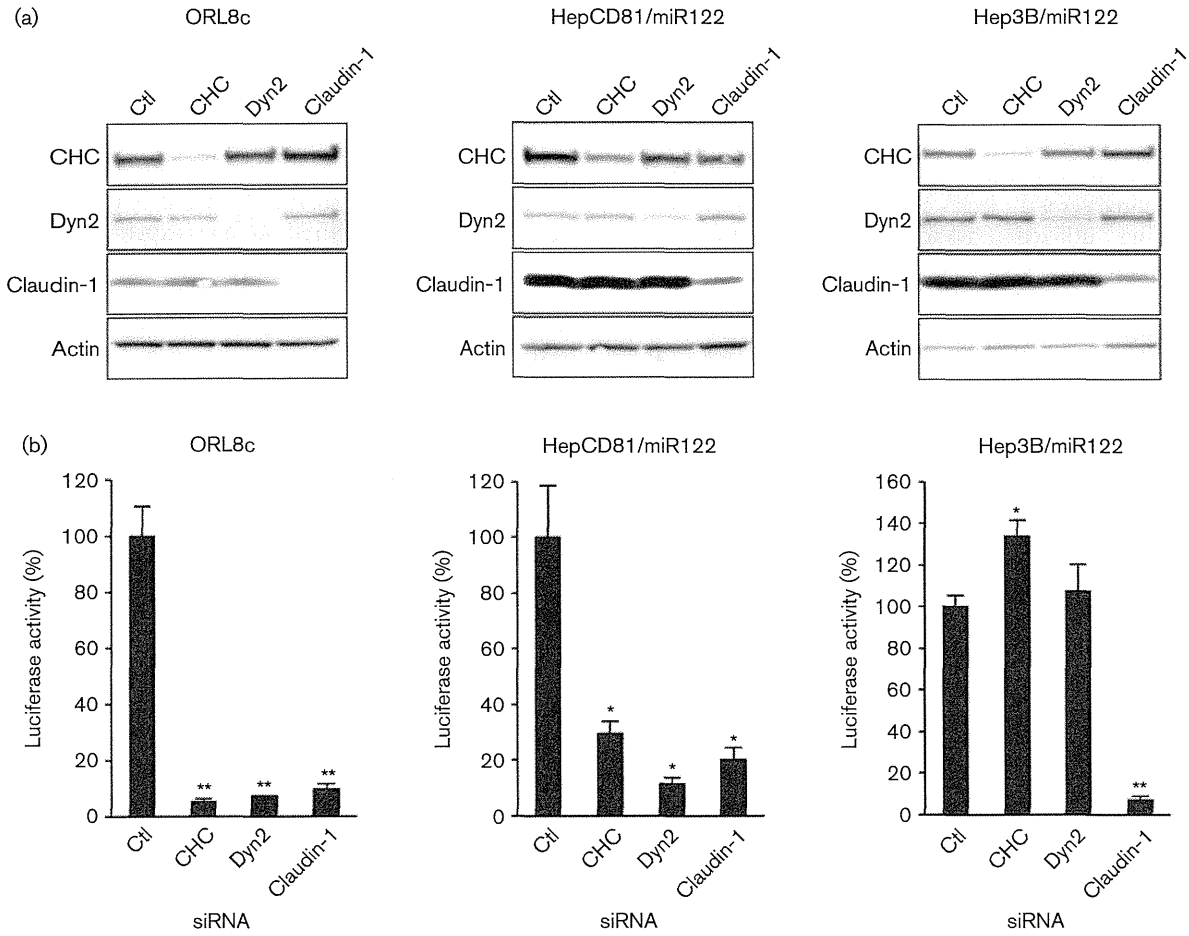

Fig. 6. Clathrin-dependent and -independent pathway of HCV entry in other HCV-permissive cells. The indicated cells were transfected with the indicated siRNAs and then infected with HCVtcp at 48 h post-transfection. (a) Specific knockdown of each protein was verified by immunoblotting. (b) Luciferase activity was determined at 72 h post-infection and expressed relative to the amount observed in the control (Ctl) siRNA transfection. Data represent the mean ± SD. Statistical differences between controls and each siRNA were evaluated using Student's *t*-test. **P*<0.05, ***P*<0.001 versus control.

In summary, we identified an alternative clathrin- and dynamin-independent entry pathway for HCV in at least two independent cell lines, Huh7.5.1 and Hep3B/miR122 cells, in addition to the previously reported clathrin- and dynamin-dependent pathway. These findings provided clues for understanding the molecular mechanisms of the endocytosis pathway for HCV infection.

DISCUSSION

Many viruses have been shown to utilize a number of different endocytic pathways to productively infect their hosts. Clathrin-dependent endocytosis would appear to be the most commonly used, but it is increasingly clear that a number of clathrin-independent endocytosis pathways are also used by several different viruses (Mercer *et al.*, 2010). In the case of HCV, it has been reported that viral entry is mediated by clathrin-dependent endocytosis (Blanchard *et al.*, 2006; Codran *et al.*, 2006; Coller *et al.*, 2009; Meertens *et al.*, 2006; Trotard *et al.*, 2009). In these papers, HCVpp was used at least in part for analysis of HCV entry pathway. However, recent reports have revealed several different characteristics between HCVpp and HCVcc.

Viral entry has been addressed primarily by pharmacologic inhibitor studies, immunofluorescence and electron microscopy, by transfection with dominant-negative constructs, and more recently by siRNA knockdown. Analysis of endocytosis pathways using pharmacological inhibitors has raised concerns about specificity. For example, chlorpromazine, an inhibitor of clathrin-mediated endocytosis, has been shown to exert multiple side-effects on cell function as it targets numerous receptors and intracellular enzymes, and alters plasma membrane characteristics (Sieczkarski & Whittaker, 2002a). Methods for elucidating the viral endocytosis pathway by co-localization of virus particles with host factor also have limitations. Electron and

fluorescence microscopy, which require a high particle number, do not allow the differentiation of infectious and non-infectious particles. Infectious particles of HCV in the supernatant of infected cells appeared to represent only a small portion of secreted virus particles (Akazawa *et al.*, 2008) and it is unclear whether the viral particles observed by microscopy could lead to productive infection. Therefore, we utilized HCVtcp, which is useful for determining productive entry of the virus without reinfection, and a combination of siRNA knockdown and dominant-negative mutants for analysis of the productive route of infection. Although HCVcc is also utilized in analysis of productive entry, it cannot completely exclude the effects of reinfection by virus produced by infected cells. Reduction of HCVcc infection by knockdown of CHC and Dyn2 was moderate when compared with that of HCVtcp (Fig. 3c, d), thus suggesting slight effects due to reinfection in HCVcc.

The data presented here demonstrate for the first time to our knowledge that HCV is able to enter cells via dynamin-independent endocytosis in addition to the previously described classical clathrin- and dynamin-dependent pathway. First, knockdown of CHC and Dyn2 had no inhibitory effects on HCVtcp and HCVcc entry into Huh7.5.1 cells. Second, overexpression of dominant-negative Dyn2 had no inhibitory effects on HCVtcp in Huh7.5.1 cells. Finally, in addition to Huh7.5.1 cells, Hep3B/miR122 cells were also shown to be infected with HCV via clathrin- and dynamin-independent pathways. We further investigated the role of alternative minor routes of HCV entry into Huh7.5.1 cells; however, the productive endocytosis pathway could not be defined. It should be noted that inhibition of alternative endocytosis routes by siRNA led to an increase of luciferase activity (Figs 3c and 5a, c). This could be explained by the inhibition of a particular endocytosis pathway resulting in a compensatory increase in alternative endocytosis pathways (Damke *et al.*, 1995).

Although we confirmed an alternative endocytosis pathway for the productive entry of HCV, it is not clear why and how the two independent endocytosis pathways operate in different cell lines. SV40 can enter cells via caveolae-dependent (Norkin *et al.*, 2002; Pelkmans *et al.*, 2001) and -independent (Damm *et al.*, 2005) pathways. Influenza virus enters cells via clathrin-mediated endocytosis (Matlin *et al.*, 1981) in addition to non-clathrin-mediated, non-caveola-mediated internalization pathways (Sieczkarski & Whittaker, 2002b). Entry of dengue virus type 2 is clathrin-dependent in HeLa and C6/36 cells (Acosta *et al.*, 2008; Mosso *et al.*, 2008; van der Schaar *et al.*, 2008), and is clathrin-independent in Vero cells (Acosta *et al.*, 2009). Different receptor usage may determine the consequential route of entry. However, we did not observe any differences between Huh-7 and Huh7.5.1 cells in terms of knockdown effects of receptor candidate molecules on HCV infection, as shown in Fig. 1(c), although we cannot exclude the possibility that other undefined receptors are associated with viral entry. Huh7.5.1 cells were established by elimination of the HCV genome from replicon cells derived from Huh-7 cells (Blight *et al.*, 2002; Zhong *et al.*, 2005) and they exhibit more potent replication of HCV than the original Huh-7 cells. Further study showed that the increased permissiveness of cured cells results from a mutation in the retinoic acid-inducible gene I (Sumpter *et al.*, 2005), which impairs IFN signalling. In addition, it has been shown that cured cell lines express higher levels of miR122 than parental cells participating in the efficient propagation of HCVcc (Kambara *et al.*, 2012). As it is unclear whether these changes are the reason for a distinct endocytosis pathway, it will be of interest to explore these associations in further studies.

In conclusion, we confirmed an alternative clathrin-independent endocytosis pathway in HCV-permissive human hepatic-derived cells, in addition to the previously reported clathrin-dependent endocytosis pathway. This paper highlights the fact that clathrin- and dynamin-mediated endocytosis is the main route of HCV entry for Huh-7, HepCD81/miR122 and ORL8c cells, whilst clathrin and dynamin do not play a major role during the productive route of HCV infection in Huh7.5.1 and Hep3B/miR122 cells. Taken together, these studies suggest that different cell entry pathways for HCV infection may be utilized in different cell types, although further studies are necessary in order to understand this phenomenon.

METHODS

Cells. The human hepatocellular carcinoma cell lines Huh-7, Huh7.5.1, Hep3B/miR122 and HepG2/CD81, which overexpressed miR122 (Kambara *et al.*, 2012), were maintained in Dulbecco's modified Eagle's medium (DMEM; Wako Pure Chemical Industries) containing non-essential amino acids, penicillin (100 U ml^{-1}), streptomycin (100 μg ml^{-1}) and 10 % FBS. Li23-derived ORL8c cells (Kato *et al.*, 2009) were maintained in F12 medium and DMEM (1 : 1, v/v) supplemented with 1 % FBS, epidermal growth factor (50 ng ml^{-1}), insulin (10 μg ml^{-1}), hydrocortisone (0.36 μg ml^{-1}), transferrin (5 μg ml^{-1}), linoleic acid (5 μg ml^{-1}), selenium (20 ng ml^{-1}), prolactin (10 ng ml^{-1}), gentamicin (10 μg ml^{-1}), kanamycin monosulfate (0.2 mg ml^{-1}) and fungizone (0.5 μg ml^{-1}). All cell lines were cultured at 37 °C in a 5 % CO_2 incubator.

Preparation of viruses. HCVtcp and HCVcc derived from JFH-1 with adaptive mutations in E2 (N417S), p7 (N765D) and NS2 (Q1012R) were generated as described previously (Suzuki *et al.*, 2012). For HepCD81/miR122 and ORL8c cells, HCVtcp containing the *Gaussia* luciferase (GLuc) reporter gene were used. To do this, plasmid pHH/SGR-JFH1/GLuc/NS3m carrying the bicistronic subgenomic HCV replicon containing the GLuc reporter gene and the NS3 adaptive mutation was constructed by replacement of the firefly luciferase (FLuc) gene of pHH/SGR-Luc containing the NS3 mutation (N1586D) (Suzuki *et al.*, 2012) with the GLuc gene of pCMV-GLuc (NEB).

Plasmids. HA-tagged Dyn2, a dominant-negative Dyn2 (K44A) in which Lys44 was replaced with Ala, was cloned into pcDNA3.1 as described previously (Kataoka *et al.*, 2012).

Gene silencing by siRNA. siRNAs were purchased from Sigma-Aldrich and were introduced into the cells at a final concentration of

30 nM using Lipofectamine RNAiMAX (Invitrogen) in accordance with the manufacturer's instructions. Target sequences of the siRNAs were: occludin (5′-GCAAGAUCACUAUGAGACA-3′), SR-BI (5′-GAGCUUUGGCCUUGGUCUA-3′), CD81 (5′-CUGUGAUCAUGAUCUUCGA-3′), CHC (5′-CUAGCUUUGCACAGUUUAA-3′), Dyn2 (5′-CCCUCAAGGAGGCGCUCAA-3′), Cav1 (5′-CCCUAAACACCUCAACGAU-3′), flotillin-1 (5′-CCUAUGACAUCGAGGUCAA-3′), Arf6 (5′-CAGUUCUUGGUAAAGUCCU-3′), CtBP1 (5′-GACUCGACGCUGUGCCACA-3′) and PAK1 (5′-GCAUCAAUUCCUGAAGAUU-3′). Target sequences of the siRNAs for claudin-1, PI4K and scrambled negative control were as described previously (Suzuki *et al.*, 2013).

Immunoblotting. Cells were washed with PBS and incubated with passive lysis buffer (Promega). Lysates were sonicated for 10 min and added to the same volume of 2× SDS-PAGE sample buffer. Protein samples were boiled for 10 min, separated by SDS-PAGE and then transferred to PVDF membranes (Merck Millipore). After blocking, membranes were probed with primary antibodies, followed by incubation with peroxidase-conjugated secondary antibody. Antigen–antibody complexes were visualized using an enhanced chemiluminescence detection system (SuperSignal West Pico Chemiluminescent Substrate; Thermo Scientific) in accordance with the manufacturer's protocols.

Flow cytometry. Cultured cells detached by treatment with trypsin were incubated with anti-CD81 antibody or anti-mouse IgG antibody for 1 h at 4 °C. After being washed with PBS containing 0.1 % BSA, cells were incubated with an Alexa Fluor 488-conjugated anti-mouse secondary antibody (Invitrogen) for 1 h at 4 °C, washed repeatedly and resuspended in PBS. Analyses were performed using a FACSCalibur system (Becton Dickinson).

Reagents and antibodies. Bafilomycin A1 was obtained from Wako Pure Chemical Industries. Alexa Fluor 488-conjugated transferrin was obtained from Invitrogen. For immunoblotting, anti-SR-BI (NB400-104; Novus Biologicals), anti-occludin (71-1500; Invitrogen), anti-claudin-1 (51-9000; Invitrogen), anti-Dyn2 (ab3457; Abcam), anti-Cav1 (N-20; Santa Cruz Biotechnology), anti-flotillin (H-104; Santa Cruz Biotechnology), anti-Arf6 (ab77581; Abcam) and anti-PAK1 (2602; Cell Signaling Technology) rabbit polyclonal antibodies; anti-CD81 (JS-81; BD Biosciences), anti-β-actin (AC-15; Sigma-Aldrich), anti-CHC (23; BD Biosciences), anti-GRAF1 (SAB1400439; Sigma-Aldrich) and anti-glyceraldehyde 3-phosphate dehydrogenase (6C5; Merck Millipore) mouse mAb; and anti-CtBP1 goat polyclonal antibody (C-17; Santa Cruz Biotechnology) were used. For immunofluorescence staining, anti-CHC mAb (X22) and anti-HA rat polyclonal antibody (3F10) were obtained from Thermo Scientific and Roche Applied Science, respectively. Anti-NS5A antibody was a rabbit polyclonal antibody against synthetic peptides. Alexa Fluor 488- or 555-labelled secondary antibodies were obtained from Invitrogen.

DNA transfection. Cell monolayers were transfected with plasmid DNA using TransIT-LT1 transfection reagent (Mirus) in accordance with the manufacturer's instructions.

Treatment of cells with bafilomycin A1 and cell viability. Cells were preincubated with various concentrations of bafilomycin A1 for 60 min at 37 °C. Preincubated cells were then infected with HCVtcp. Cells treated with 0.1 % DMSO were used as controls. Cell viability was analysed by the Cell Titre-Glo Luminescent Cell Viability Assay (Promega).

Uptake of transferrin. Cells were grown on glass coverslips. After cells were transfected with HA-tagged Dyn2 expression plasmids, Alexa Fluor 488-conjugated transferrin at 20 μg ml^{-1} was added and incubated for 30 min. Cells were washed with PBS and fixed in 4 % paraformaldehyde.

Immunofluorescence analysis. Huh7.5.1 and Huh-7 cells were fixed with 4 % paraformaldehyde in PBS for 30 min, and were then blocked and permeabilized with 0.3 % Triton X-100 in a non-fat milk solution (Block Ace; Snow Brand Milk Products) for 60 min at room temperature. Samples were then incubated with anti-CHC, anti-Dyn2, anti-Cav1, anti-NS5A or anti-HA for 60 min at room temperature, washed three times with PBS, and then incubated with secondary antibodies for 60 min at room temperature. Finally, samples were washed three times with PBS, rinsed briefly in double-distilled H_2O and mounted with DAPI mounting medium. The signal was analysed using a Leica TCS SPE confocal microscope.

Luciferase assay. For quantification of FLuc activity in HCVtcp-infected cells, cells were lysed with passive lysis buffer (Promega) at 72 h post-infection. FLuc activity of the cells was determined using a luciferase assay system (Promega). For quantification of GLuc activity in supernatants of HCVtcp-infected cells, the *Renilla* Luciferase Assay System (Promega) was used. All luciferase assays were performed at least in triplicate.

Quantification of HCV core protein. HCV core protein was quantified using a highly sensitive enzyme immunoassay (Lumipulse G1200; Fujirebio) in accordance with the manufacturer's instructions.

ACKNOWLEDGEMENTS

We are grateful to Francis V. Chisari (Scripps Research Institute) for providing Huh-7 and Huh7.5.1 cells. We would also like to thank M. Sasaki for technical assistance, and T. Kato, A. Murayama and K. Mori for helpful discussion.

REFERENCES

Acosta, E. G., Castilla, V. & Damonte, E. B. (2008). Functional entry of dengue virus into *Aedes albopictus* mosquito cells is dependent on clathrin-mediated endocytosis. *J Gen Virol* **89**, 474–484.

Acosta, E. G., Castilla, V. & Damonte, E. B. (2009). Alternative infectious entry pathways for dengue virus serotypes into mammalian cells. *Cell Microbiol* **11**, 1533–1549.

Akazawa, D., Date, T., Morikawa, K., Murayama, A., Omi, N., Takahashi, H., Nakamura, N., Ishii, K., Suzuki, T. & other authors (2008). Characterization of infectious hepatitis C virus from liver-derived cell lines. *Biochem Biophys Res Commun* **377**, 747–751.

Bartosch, B., Vitelli, A., Granier, C., Goujon, C., Dubuisson, J., Pascale, S., Scarselli, E., Cortese, R., Nicosia, A. & Cosset, F. L. (2003). Cell entry of hepatitis C virus requires a set of co-receptors that include the CD81 tetraspanin and the SR-B1 scavenger receptor. *J Bio Chem* **278**, 41624–41630.

Benedicto, I., Molina-Jimenez, F., Bartosch, B., Cosset, F. L., Lavillette, D., Prieto, J., Moreno-Otero, R., Valenzuela-Fernandez, A., Aldabe, R., Lopez-Cabrera, M. & Majano, P. L. (2009). The tight junction-associated protein occludin is required for a postbinding step in hepatitis C virus entry and infection. *J Virol* **83**, 8012–8020.

Blanchard, E., Belouzard, S., Goueslain, L., Wakita, T., Dubuisson, J., Wychowski, C. & Rouillé, Y. (2006). Hepatitis C virus entry depends on clathrin-mediated endocytosis. *J Virol* **80**, 6964–6972.

Blight, K. J., McKeating, J. A. & Rice, C. M. (2002). Highly permissive cell lines for subgenomic and genomic hepatitis C virus RNA replication. *J Virol* **76**, 13001–13014.

Codran, A., Royer, C., Jaeck, D., Bastien-Valle, M., Baumert, T. F., Kieny, M. P., Pereira, C. A. & Martin, J. P. (2006). Entry of hepatitis C

virus pseudotypes into primary human hepatocytes by clathrin-dependent endocytosis. *J Gen Virol* **87**, 2583–2593.

Coller, K. E., Berger, K. L., Heaton, N. S., Cooper, J. D., Yoon, R. & Randall, G. (2009). RNA interference and single particle tracking analysis of hepatitis C virus endocytosis. *PLoS Pathog* **5**, e1000702.

Damke, H., Baba, T., van der Bliek, A. M. & Schmid, S. L. (1995). Clathrin-independent pinocytosis is induced in cells overexpressing a temperature-sensitive mutant of dynamin. *J Cell Biol* **131**, 69–80.

Damm, E. M., Pelkmans, L., Kartenbeck, J., Mezzacasa, A., Kurzchalia, T. & Helenius, A. (2005). Clathrin- and caveolin-1-independent endocytosis: entry of simian virus 40 into cells devoid of caveolae. *J Cell Biol* **168**, 477–488.

Evans, M. J., von Hahn, T., Tscherne, D. M., Syder, A. J., Panis, M., Wolk, B., Hatziioannou, T., McKeating, J. A., Bieniasz, P. D. & Rice, C. M. (2007). Claudin-1 is a hepatitis C virus co-receptor required for a late step in entry. *Nature* **446**, 801–805.

Grove, J. & Marsh, M. (2011). The cell biology of receptor-mediated virus entry. *J Cell Biol* **195**, 1071–1082.

Grove, J., Nielsen, S., Zhong, J., Bassendine, M. F., Drummer, H. E., Balfe, P. & McKeating, J. A. (2008). Identification of a residue in hepatitis C virus E2 glycoprotein that determines scavenger receptor BI and CD81 receptor dependency and sensitivity to neutralizing antibodies. *J Virol* **82**, 12020–12029.

Helle, F., Vieyres, G., Elkrief, L., Popescu, C.-I., Wychowski, C., Descamps, V., Castelain, S., Roingeard, P., Duverlie, G. & Dubuisson, J. (2010). Role of N-linked glycans in the functions of hepatitis C virus envelope proteins incorporated into infectious virions. *J Virol* **84**, 11905–11915.

Hoofnagle, J. H. (2002). Course and outcome of hepatitis C. *Hepatology* **36** (Suppl 1), S21–S29.

Kambara, H., Fukuhara, T., Shiokawa, M., Ono, C., Ohara, Y., Kamitani, W. & Matsuura, Y. (2012). Establishment of a novel permissive cell line for the propagation of hepatitis C virus by expression of microRNA miR122. *J Virol* **86**, 1382–1393.

Kataoka, C., Kaname, Y., Taguwa, S., Abe, T., Fukuhara, T., Tani, H., Moriishi, K. & Matsuura, Y. (2012). Baculovirus GP64-mediated entry into mammalian cells. *J Virol* **86**, 2610–2620.

Kato, N., Mori, K., Abe, K., Dansako, H., Kuroki, M., Ariumi, Y., Wakita, T. & Ikeda, M. (2009). Efficient replication systems for hepatitis C virus using a new human hepatoma cell line. *Virus Res* **146**, 41–50.

Liu, S., Yang, W., Shen, L., Turner, J. R., Coyne, C. B. & Wang, T. (2009). Tight junction proteins claudin-1 and occludin control hepatitis C virus entry and are downregulated during infection to prevent superinfection. *J Virol* **83**, 2011–2014.

Lupberger, J., Zeisel, M. B., Xiao, F., Thumann, C., Fofana, I., Zona, L., Davis, C., Mee, C. J., Turek, M. & other authors (2011). EGFR and EphA2 are host factors for hepatitis C virus entry and possible targets for antiviral therapy. *Nat Med* **17**, 589–595.

Marsh, M. & Helenius, A. (2006). Virus entry: open sesame. *Cell* **124**, 729–740.

Matlin, K. S., Reggio, H., Helenius, A. & Simons, K. (1981). Infectious entry pathway of influenza virus in a canine kidney cell line. *J Cell Biol* **91**, 601–613.

McKeating, J. A., Zhang, L. Q., Logvinoff, C., Flint, M., Zhang, J., Yu, J., Butera, D., Ho, D. D., Dustin, L. B., Rice, C. M. & Balfe, P. (2004). Diverse hepatitis C virus glycoproteins mediate viral infection in a CD81-dependent manner. *Journal of virology* **78**, 8496–8505.

Meertens, L., Bertaux, C. & Dragic, T. (2006). Hepatitis C virus entry requires a critical postinternalization step and delivery to early endosomes via clathrin-coated vesicles. *J Virol* **80**, 11571–11578.

Mercer, J., Schelhaas, M. & Helenius, A. (2010). Virus entry by endocytosis. *Annu Rev Biochem* **79**, 803–833.

Miaczynska, M. & Stenmark, H. (2008). Mechanisms and functions of endocytosis. *J Cell Biol* **180**, 7–11.

Mosso, C., Galván-Mendoza, I. J., Ludert, J. E. & del Angel, R. M. (2008). Endocytic pathway followed by dengue virus to infect the mosquito cell line C6/36 HT. *Virology* **378**, 193–199.

Norkin, L. C., Anderson, H. A., Wolfrom, S. A. & Oppenheim, A. (2002). Caveolar endocytosis of simian virus 40 is followed by brefeldin A-sensitive transport to the endoplasmic reticulum, where the virus disassembles. *J Virol* **76**, 5156–5166.

Pelkmans, L., Kartenbeck, J. & Helenius, A. (2001). Caveolar endocytosis of simian virus 40 reveals a new two-step vesicular-transport pathway to the ER. *Nat Cell Biol* **3**, 473–483.

Pileri, P., Uematsu, Y., Campagnoli, S., Galli, G., Falugi, F., Petracca, R., Weiner, A. J., Houghton, M., Rosa, D., Grandi, G. & Abrignani, S. (1998). Binding of hepatitis C virus to CD81. *Science* **282**, 938–941.

Ploss, A., Evans, M. J., Gaysinskaya, V. A., Panis, M., You, H., de Jong, Y. P. & Rice, C. M. (2009). Human occludin is a hepatitis C virus entry factor required for infection of mouse cells. *Nature* **457**, 882–886.

Sainz, B., Jr, Barretto, N., Martin, D. N., Hiraga, N., Imamura, M., Hussain, S., Marsh, K. A., Yu, X., Chayama, K. & other authors (2012). Identification of the Niemann–Pick C1-like 1 cholesterol absorption receptor as a new hepatitis C virus entry factor. *Nat Med* **18**, 281–285.

Scarselli, E., Ansuini, H., Cerino, R., Roccasecca, R. M., Acali, S., Filocamo, G., Traboni, C., Nicosia, A., Cortese, R. & Vitelli, A. (2002). The human scavenger receptor class B type I is a novel candidate receptor for the hepatitis C virus. *Embo J* **21**, 5017–5025.

Sieczkarski, S. B. & Whittaker, G. R. (2002a). Dissecting virus entry via endocytosis. *J Gen Virol* **83**, 1535–1545.

Sieczkarski, S. B. & Whittaker, G. R. (2002b). Influenza virus can enter and infect cells in the absence of clathrin-mediated endocytosis. *J Virol* **76**, 10455–10464.

Sumpter, R., Jr, Loo, Y.-M., Foy, E., Li, K., Yoneyama, M., Fujita, T., Lemon, S. M. & Gale, M., Jr (2005). Regulating intracellular antiviral defense and permissiveness to hepatitis C virus RNA replication through a cellular RNA helicase, RIG-I. *J Virol* **79**, 2689–2699.

Suzuki, T., Ishii, K., Aizaki, H. & Wakita, T. (2007). Hepatitis C viral life cycle. *Adv Drug Deliv Rev* **59**, 1200–1212.

Suzuki, R., Saito, K., Kato, T., Shirakura, M., Akazawa, D., Ishii, K., Aizaki, H., Kanegae, Y., Matsuura, Y. & other authors (2012). Trans-complemented hepatitis C virus particles as a versatile tool for study of virus assembly and infection. *Virology* **432**, 29–38.

Suzuki, R., Matsuda, M., Watashi, K., Aizaki, H., Matsuura, Y., Wakita, T. & Suzuki, T. (2013). Signal peptidase complex subunit 1 participates in the assembly of hepatitis C virus through an interaction with E2 and NS2. *PLoS Pathog* **9**, e1003589.

Trotard, M., Lepère-Douard, C., Régeard, M., Piquet-Pellorce, C., Lavillette, D., Cosset, F. L., Gripon, P. & Le Seyec, J. (2009). Kinases required in hepatitis C virus entry and replication highlighted by small interference RNA screening. *FASEB J* **23**, 3780–3789.

van der Schaar, H. M., Rust, M. J., Chen, C., van der Ende-Metselaar, H., Wilschut, J., Zhuang, X. & Smit, J. M. (2008). Dissecting the cell entry pathway of dengue virus by single-particle tracking in living cells. *PLoS Pathog* **4**, e1000244.

Vieyres, G., Thomas, X., Descamps, V., Duverlie, G., Patel, A. H. & Dubuisson, J. (2010). Characterization of the envelope glycoproteins associated with infectious hepatitis C virus. *J Virol* **84**, 10159–10168.

Zhong, J., Gastaminza, P., Cheng, G., Kapadia, S., Kato, T., Burton, D. R., Wieland, S. F., Uprichard, S. L., Wakita, T. & Chisari, F. V. (2005). Robust hepatitis C virus infection *in vitro*. *Proc Natl Acad Sci U S A* **102**, 9294–9299.

Journal of Virological Methods 207 (2014) 38–44

Contents lists available at ScienceDirect

Journal of Virological Methods

journal homepage: www.elsevier.com/locate/jviromet

Characterization of human bocavirus-like particles generated by recombinant baculoviruses

Ling Fang[a], Zejun Wang[b], Shili Song[c], Michiyo Kataoka[f], Changwen Ke[a], Tetsuro Suzuki[d], Takaji Wakita[g], Naokazu Takeda[e], Tian-Cheng Li[g,*]

[a] Institute of Pathogenic Microbiology, Center for Disease Control and Prevention of Guangdong Province, 160 Qunxian Road, Dashi Street, Panyu District, Guangzhou 511430, China
[b] Department of Genetic Engineering, Wuhan Institute of Biological Products (WIBP), Linjiang Avenue, Wuchang, Wuhan, 430060, China
[c] Institute of Microbiology, Yuhang Center for Disease Control and Prevention, 930 Shijidadao Avenue, Hangzhou 311100, China
[d] Department of Infectious Diseases, Hamamatsu University School of Medicine, 1-20-1 Handayama, Higashi-ku, Hamamatsu 431-3192, Japan
[e] Research Institute for Microbial Diseases, Osaka University, Suita 565-0781, Osaka, Japan
[f] Department of Pathology, National Institute of Infectious Diseases, Gakuen 4-7-1, Musashi-murayama 208-0011, Tokyo, Japan
[g] Department of Virology II, National Institute of Infectious Diseases, Gakuen 4-7-1, Musashi-murayama 208-0011, Tokyo, Japan

Article history:
Received 11 March 2014
Received in revised form 4 June 2014
Accepted 6 June 2014
Available online 30 June 2014

Keywords:
Human bocaviruses
HBoV1–4
Recombinant baculovirus
Virus-like particles
VLP
Insect cells Tn5 and Sf9

ABSTRACT

Human bocavirus (HBoV) is a nonenveloped, single-stranded DNA virus, classified recently into the genus *Bocavirus* in the family *Parvoviridae*. A recombinant baculovirus expression system was used to express the major capsid protein VP2 of HBoV1, HBoV2, HBoV3 and HBoV4 in insect cells. A large amount of the 61-kDa VP2 capsid protein (p61) of HBoVs was generated and efficiently released into the supernatant. The capsid protein was self-assembled into 22-nm-dia. virus-like particles (VLPs) with a buoyant density of 1.30 g/cm^3. The morphology of HBoVs-LPs was similar to that of the native HBoV particles, and immunogenic studies demonstrated the cross-reactivity among HBoV1, HBoV2, HBoV3 and HBoV4. When VP1 and VP2 protein of HBoV1 were co-expressed in insect cells, both proteins were detected in the same fraction after CsCl gradient centrifugation, suggesting that the VP1 protein is a minor structural protein of HBoVs. We developed an ELISA using purified VLPs as the antigen and used it to detect antibodies against HBoV1, HBoV2, HBoV3 and HBoV4. A high prevalence of antibodies against HBoVs was found in a general population of healthy Japanese, indicating that HBoVs have spread throughout Japan.

1. Introduction

Human bocavirus type 1 (HBoV1), HBoV2, HBoV3 and HBoV4 are members of the genus *Bocavirus* in the subfamily *Parvovirinae* of the family *Parvoviridae* (Jartti et al., 2012). Following the first identification of HBoV1 in the nasopharyngeal secretion of a child with respiratory manifestations in 2005 (Allander et al., 2005), HBoV2, HBoV3 and HBoV4 were identified in fecal samples from children with non-polio acute flaccid paralysis and diarrhea in 2009 and 2010 (Arthur et al., 2009; Kapoor et al., 2009, 2010). HBoV is a small, nonenveloped icosahedral virus with a linear, single-stranded DNA genome of approx. 5.3 kilobases (kb). Sequence analyses of the HBoV genome revealed that it contains three open reading frames (ORFs) encoding four proteins in the following order: two nonstructural proteins (NS1 and NP1) and two viral capsid proteins (VP1 and VP2) (Allander et al., 2005). As in other members of the family *Parvoviridae*, the two capsid proteins, VP1 and VP2, have identical nucleotide and amino acid sequences except for an extra unique phospholipase-A motif (VP1u) at the amino-terminal end of the VP1 protein (Dijkman et al., 2009; Chen et al., 2010). The capsid protein exhibits $T=1$ symmetry with 60 copies of the coat protein (Gurda et al., 2010). The functions of NS1 and NP1 are unknown.

HBoV infection is associated mainly with pediatric respiratory diseases and gastrointestinal diseases (Jartti et al., 2012). HBoV DNAs have been detected in 5% to 15% of patients with respiratory illness or gastrointestinal symptoms in North America, South America, Europe, Asia, Australia and Africa, indicating that HBoV infection is a global health concern (Longtin et al., 2008; Arthur et al., 2009; Fabbiani et al., 2009; Moreno et al., 2009; Soderlund-Venermo et al., 2009; Tozer et al., 2009; Vallet et al., 2009; Chow et al., 2010; Huang et al., 2010; Kapoor et al., 2009, 2010; Santos et al., 2010). The lack of an efficient cell culture system for HBoV has hampered the preparation of antigens for the serology assay. It is generally accepted that noninfectious virus-like particles (VLPs)

* Corresponding author. Tel.: +81 42 561 0771; fax: +81 42 561 4729.
E-mail address: litc@nih.go.jp (T.-C. Li).

http://dx.doi.org/10.1016/j.jviromet.2014.06.007
0166-0934/

assembled from the viral structural proteins are similar to native virions in size, shape and antigenicity, and thus that VLPs are useful as antigens for immunoassays.

To understand the antigenic properties of HBoVs, we established an efficient production system for HBoV1–4 VLPs using a recombinant baculovirus expression system, and we characterized the antigenicity of the purified VLPs. We performed seroepidemiological studies on HBoVs with sera from healthy populations in Japan using an enzyme-linked immunosorbent assay (ELISA) that was developed based on VLPs as the antigen.

2. Materials and methods

2.1. Construction of recombinant baculoviruses and expression of HBoV capsid proteins

We synthesized the viral genes encoding VP1 of HBoV1, VP2 of HBoV1, VP2 of HBoV2, VP2 of HBoV3 and VP2 of HBoV4, each of which contains a *Bam*HI site before the start codon and an *Xba*I site after the stop codon, based on published sequences (GenBank accession nos.: AB481080, FJ170279, FJ948861, and NC_012729), and cloned them into vector pUC57 (GeneScript, Piscataway, NJ) to generate plasmids pUC57-HBoV1-VP1, pUC57-HBoV1-VP2, pUC57-HBoV2-VP2, pUC57-HBoV3-VP2, and pUC57-HBoV4-VP2. These plasmids were digested with *Bam*HI and *Xba*I, and the purified VP1 or VP2 gene fragment was ligated to the transfer vector pVL1393 (Pharmingen, San Diego, CA), yielding plasmids pVL1393-HBoV1-VP1, pVL1393-HBoV1-VP2, pVL1393-HBoV2-VP2, pVL1393-HBoV3-VP2, and pVL1393-HBoV4-VP2.

An insect cell line, Sf9, derived from the armyworm *Spodoptera frugiperda* (Riken Cell Bank, Tsukuba, Japan), was co-transfected with a linearized wild-type *Autographa californica* nuclear polyhedrosis virus DNA (BaculoGold 21100D; Pharmingen) and the transfer plasmid by a lipofectin-mediated method as specified by the manufacturer (GIBCO-BRL, Gaithersburg, MD). The cells were incubated at 26.5 °C in TC-100 medium (GIBCO-BRL) supplemented with 8% fetal bovine serum (FBS) and 0.26% bacto tryptose phosphate broth (Difco Laboratories, Detroit, MI). Each recombinant virus was plaque-purified three times in Sf9 cells. The baculovirus recombinants thus obtained were designated as AcHBoV1-VP1, AcHBoV1-VP2, AcHBoV2-VP2, AcHBoV3-VP2 and AcHBoV4-VP2, respectively. For large-scale expression, we used an insect cell line from the cabbage looper *Trichoplusia ni*, BTL-Tn 5B1-4 (Tn5) (Invitrogen, San Diego, CA). Tn5 cells were infected with the recombinant baculoviruses at a multiplicity of infection (m.o.i.) of 10 and cultured in EX-CELL 405 medium (JRH Biosciences, Lenexa, KS) at 26.5 °C as described (Li et al., 1997, 2011).

2.2. Sodium dodecyl sulfate-polyacrylamide gel electrophoresis (SDS-PAGE) and Western blot analysis

The proteins in the cell lysate and culture medium were separated by 5–20% sodium dodecyl sulfate-polyacrylamide gel electrophoresis (SDS-PAGE) and stained with Coomassie blue. For Western blotting, the proteins in the SDS-PAGE gel were electrophoretically transferred onto a nitrocellulose membrane. The membrane was then blocked with 50 mM Tris–HCl (pH 7.4) containing 5% skim milk and 150 mM NaCl, and incubated with a human serum positive for anti-HBoV IgG. Detection of human IgG antibody was achieved using alkaline phosphatase conjugate goat anti-human IgG (1:1000 dilution; Dako, Copenhagen, Denmark). Nitroblue tetrazolium chloride and 5-bromo-4-chloro-3-indolyl phosphate P-toluidine were used as coloring agents (Bio-Rad Laboratories, Hercules, CA).

2.3. Purification of VLPs

The culture medium of the recombinant baculovirus-infected Tn5 cells was harvested on day 7 post-infection (p.i.). The intact cells, cell debris, and progeny baculoviruses were removed by centrifugation at 10,000 × *g* for 60 min. The supernatant was then spun at 126,000 × *g* for 3 h in a rotor (SW32Ti, Beckman Coulter, Indianapolis, IN), and the resulting pellet was resuspended in EX-CELL™ 405 medium at 4 °C overnight. For the CsCl gradient centrifugation, 4.5 mL of the samples were mixed with 2.1 g of CsCl, and then centrifuged at 116,000 × *g* for 24 h at 10 °C in the SW55Ti rotor. The gradient was fractionated into 250-μL aliquots, and each fraction was weighed in order to estimate the buoyant density and isopycnic point. Each fraction was diluted with EX-CELL™ 405 medium and centrifuged for 2 h at 237,000 × *g* in a Beckman TLA55 rotor to sediment the VLPs.

2.4. Electron microscopy (EM)

The purified VLPs were placed on a carbon-coated grid for 45 s, rinsed with distilled water, stained with a 2% uranyl acetate, and examined with an electron microscope (TEM-1400, JEOL, Tokyo) at 80 kV.

2.5. N-terminal amino acid sequence analysis

VLPs were purified by CsCl gradient centrifugation. N-terminal amino acid (aa) microsequencing was carried out using 100 pmol of the protein by Edman automated degradation on a protein sequencer (model 477, Applied Biosystems, Foster City, CA).

2.6. Healthy human serum samples

The specimens tested for HBoV serology consisted of 372 serum samples from healthy Japanese subjects collected in 1993. Serum samples were obtained from the Serum Bank of the National Institute of Infectious Diseases, Japan. The ages of the subjects ranged from 1 to 80 years old. Sixty-four percent (238/372) of the subjects were female, and 36% (134/372) were male.

2.7. Hyperimmune sera

Rabbits (Japanese White, 8 weeks old, female) were immunized with VLPs. The immunization was performed by a thigh muscle injection of purified VLPs at a dose of 500 μg per animal, and the booster injections were carried out at 4 and 6 weeks after the first injection with half doses of VLPs. All of the injections including the booster injections were carried out without any adjuvant. Immunized animals were bled 1 week after the last injection. The rabbit experiments were reviewed by the National Institute of Infectious Diseases (NIID) Ethics Committee and carried out according to the "Guides for Animal Experiments Performed at NIID" under code 111054.

2.8. Enzyme-linked immunosorbent assay (ELISA)

We developed an ELISA to detect anti-HBoV antibodies in human sera. Flat-bottom 96-well polystyrene microplates (Immulon 2; Dynex Technologies, Chantilly, VA) were coated with the purified VLPs (1 μg/mL, 100 μL/well) and incubated overnight at 4 °C. Unbound VLPs were removed, and the plates were washed twice with 10-mM phosphate-buffered saline (PBS) containing 0.05% Tween 20 (PBS-T) and then blocked with 200 μL of 5% skim milk (Difco Laboratories) dissolved in PBS-T for 1 h at 37 °C. After three washes with PBS-T, diluted rabbit or human serum (100 μL/well) was added in duplicate. The plates were incubated

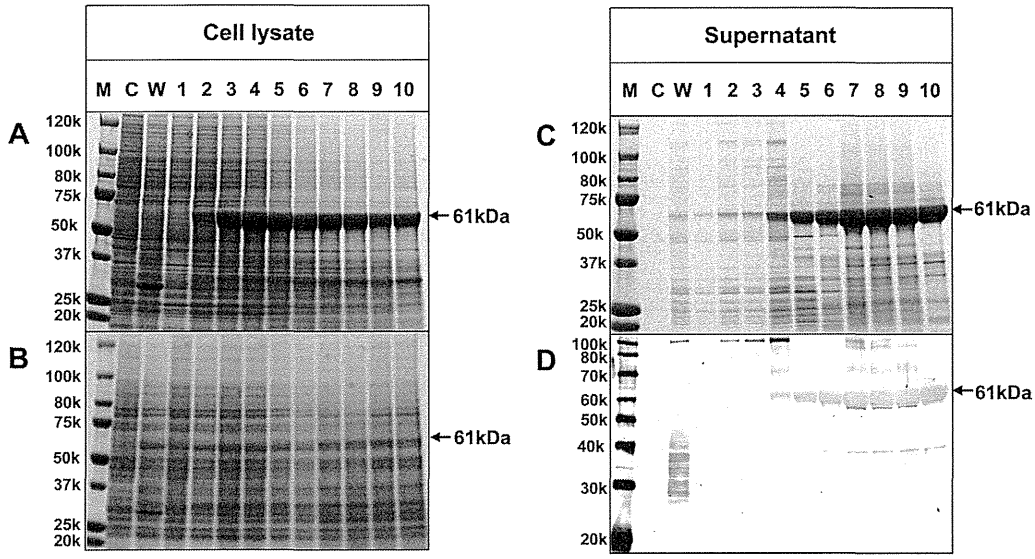

Fig. 1. Time course of HBoV1-VP2 expression. Insect cells, Tn5 ((A), (C) and (D)) and Sf9 (B), were infected with the recombinant baculovirus AcHBoV1-VP2 and incubated at 26.5 °C. The cells were harvested on the indicated days (days 1 to 10), and 5 μL of the sample from 25-times concentrated culture medium or the equivalent of the cell lysate from 10^5 cells was analyzed by SDS-PAGE. Protein bands were visualized by Coomassie blue staining or Western blot assay with an anti-HBoV1 IgG-positive human serum. (A) Coomassie blue staining of the Tn5 cell lysate. (B) Coomassie blue staining of the Sf9 cell lysate. (C) Coomassie blue staining of the Tn5 cell supernatant. (D) Western blot assay of the Tn5 cell supernatant. Arrows, p61; M, molecular weight marker; C, mock-infected cells; W, wild-type baculovirus-infected cells; lanes 1 to 10, AcHBoV1-VP2-infected Sf9 or Tn5 cells were harvested on 1 to 10 days p.i.

at 37 °C for 1 h and washed three times as described above. The wells were incubated with 100 μL of horseradish peroxidase-conjugated goat anti-human IgG (H + L) (Cappel, West Chester, PA) (1:10,000 dilution), IgM (Cappel) (1:2000 dilution) or horseradish peroxidase-conjugated goat anti-rabbit IgG (Cappel, Durham, NC) (1:2000 dilution) diluted with PBS-T containing 1% skim milk.

The plates were incubated at 37 °C for 1 h and washed four times with PBS-T. The substrate orthophenylenediamine (100 μL) (Sigma Chemical, St. Louis, MO) and H_2O_2 were added to each well. The plates were incubated in a dark room at room temperature for 30 min, then 50 μL of 4 N H_2SO_4 was added into each well. Absorbance was measured at 492 nm. Test samples were considered positive when the absorbance was ≥0.200.

2.9. Statistics method

Proportional analysis between groups and correlation analysis among anti-HBoV antibody levels were performed with the chi-squared test and Spearman test, respectively, using SPSS software.

3. Results

3.1. Efficient expression of HBoV VP2 proteins in Tn5 cells

To examine which insect cell line is suitable for the expression of HBoV capsid proteins, we used the recombinant baculovirus AcHBoV1-VP2 to infect Sf9 or Tn5 cells. The infected cells were harvested daily until 10 days p.i., and the protein expression was analyzed by SDS-PAGE followed by Coomassie blue staining. In the Tn5 cell lysates, one strong protein band with molecular mass of 61 kDa (p61) was first detected on day 2 and reached a peak on day 4 p.i. (Fig. 1A) In contrast, the expression level of VP2 in Sf9 cells was quite low, and we were unable to specify the VP2 protein by Coomassie blue staining (Fig. 1B); hence, we used Tn5 cells exclusively thereafter.

A large amount of p61 was also detected in the supernatant in infected Tn5 cells on day 4 and peaked on day 7 p.i. (Fig. 1C), suggesting that the HBoV-VP2 protein was efficiently released into the supernatant. The p61 in the supernatant reacted with human serum that was positive for anti-HBoV IgG in Western blotting (Fig. 1D). The expression level and pattern of the VP2 capsid protein of HBoV2, HBoV3 and HBoV4 were similar to those of HBoV1-VP2 (data not shown).

3.2. Recombinant VP2 of HBoV1–4 self-assembled into virus-like particles

The supernatant of recombinant baculovirus-infected Tn5 cells was harvested at 7 days p.i. and subjected to a CsCl density gradient centrifugation. The gradient was fractionated into 20 aliquots, and analyzed by SDS-PAGE followed by Coomassie blue staining. As shown in Fig. 2, p61 appeared in fraction 8 at a density of 1.30 g/cm^3

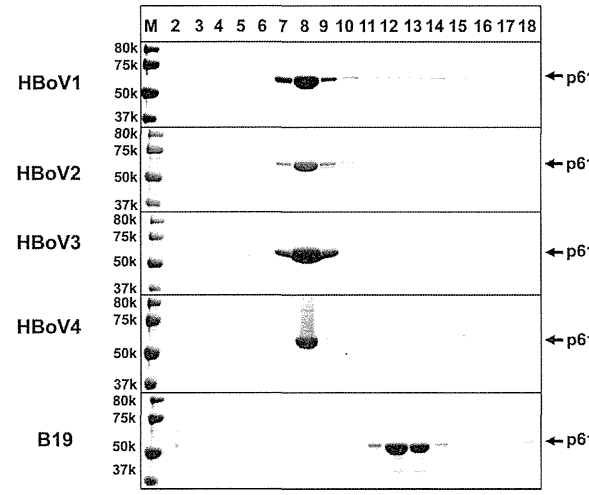

Fig. 2. Purification of HBoVLPs. The recombinant baculovirus-infected Tn5 cells were harvested on 7 day p.i., and the supernatant was centrifuged for 3 h at 32,000 rpm in a Beckman SW32Ti rotor. The pellet was resuspended in 500 μL EX-CELL™ 405, and then purified by CsCl equilibrium density gradient centrifugation. Aliquots from each fraction were analyzed by electrophoresis on 5% to 20% polyacrylamide gel, and stained with Coomassie blue.